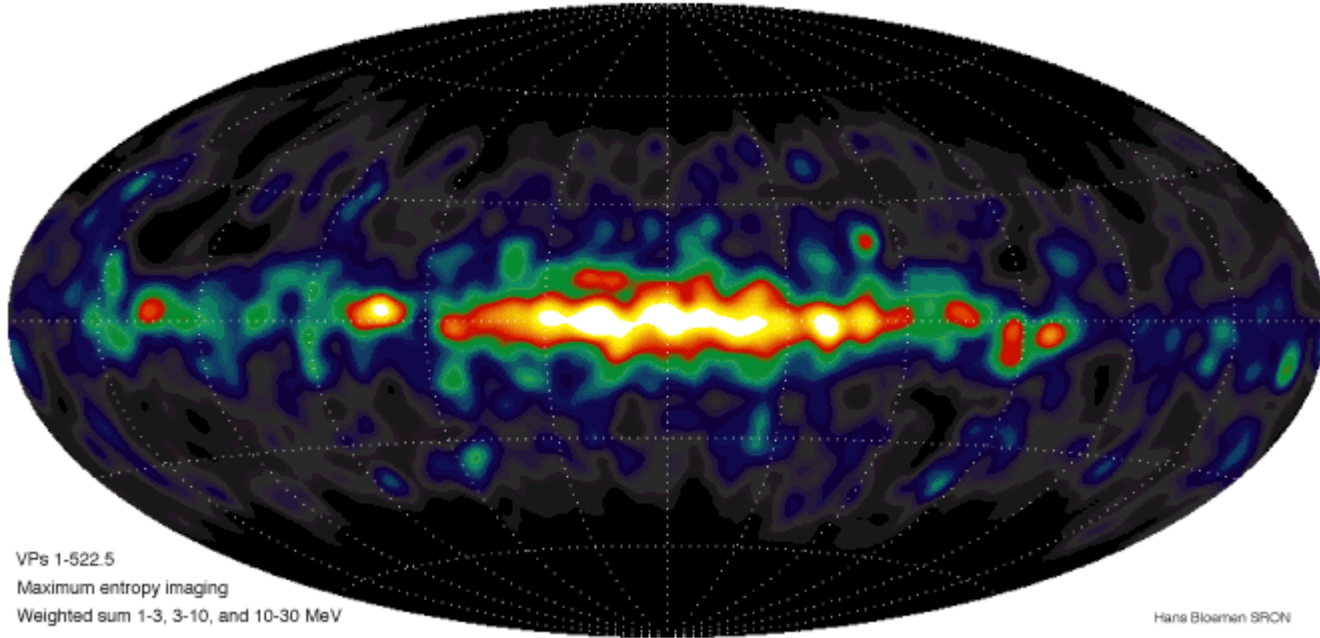


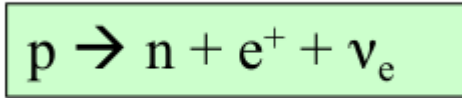
COMPTEL 1-30 MeV



Gamma-Ray Lines via Radioactive Decay

Interlude: Inverse beta decay

Very often you read about the inverse beta decay as the following reaction:

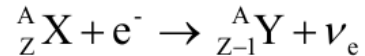


However, *free* protons *do not decay* since they are stable in the Standard Model.

Inside nuclei however, the following reaction is allowed:

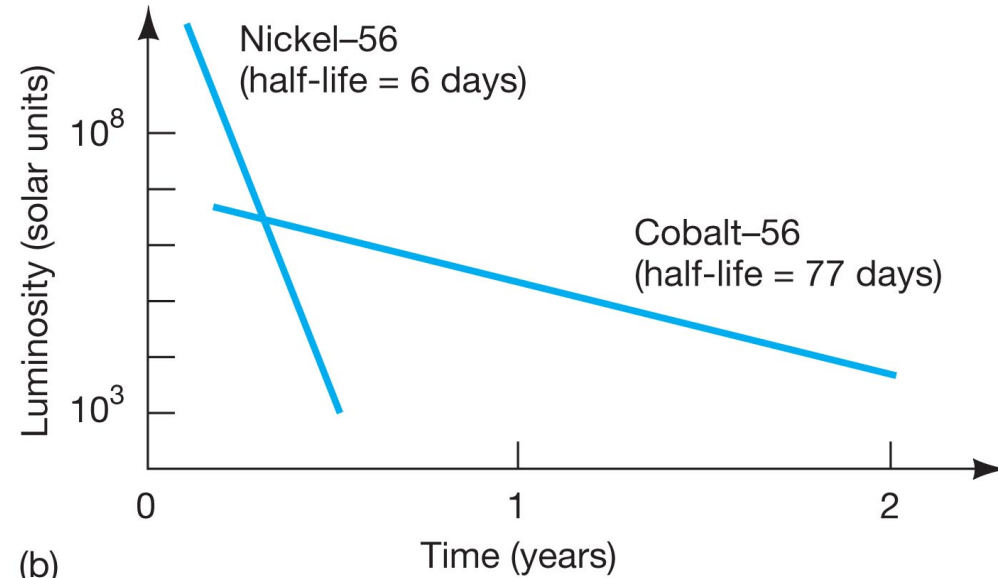
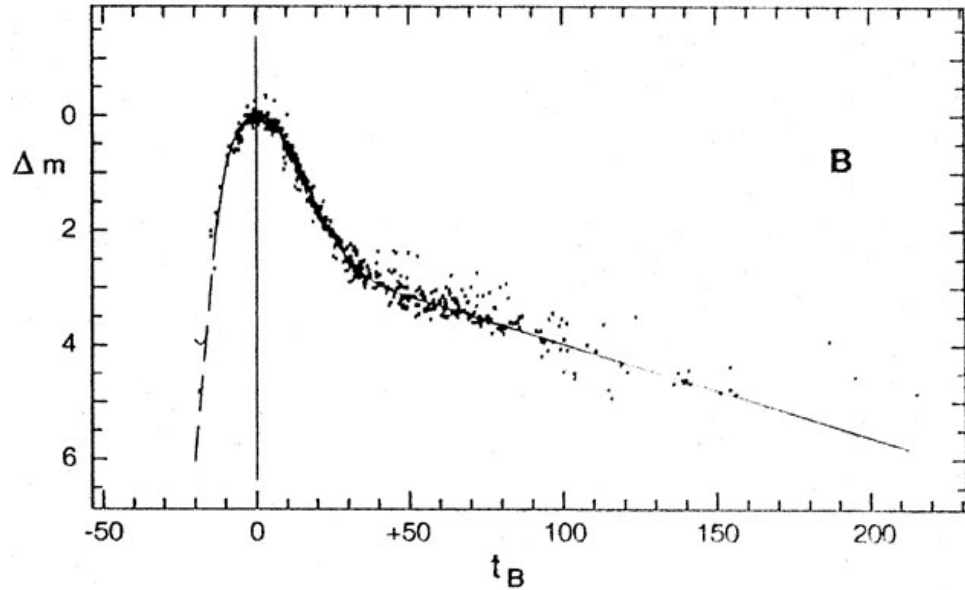


It is also possible to have inverse beta decay as **electron capture**, with no positron emission:



NOTE: If the difference in energy between two nuclei that differ by just one neutron being changed into a proton is high enough to produce an extra electron (by $E=mc^2$ the mass of this electron comes from difference in energy), then the nucleus can and will beta decay.

Supernovae Ia Lightcurve: Powered by Radioactivity



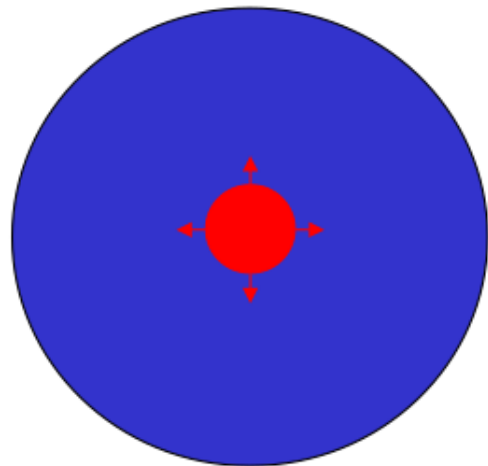
Thermonuclear supernovae (SNe Ia)

Explosion mechanism?
Scenario

CO white dwarf with Mass $\sim 1.4 M_{\odot}$:
central C-ignition



$[\text{CO} \rightarrow \text{Ni} - 7 \times 10^{17} \text{ erg/g} \rightarrow \underline{10^{51} \text{ erg}}]$



Ni from SN Ia \rightarrow origin of Galactic Fe

Optical light
curve

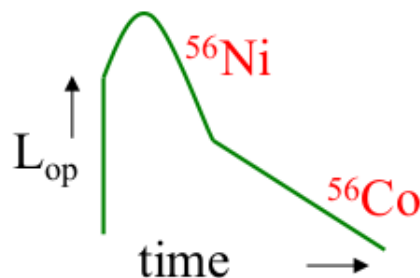


$\tau_{1/2} : 6\text{d}$

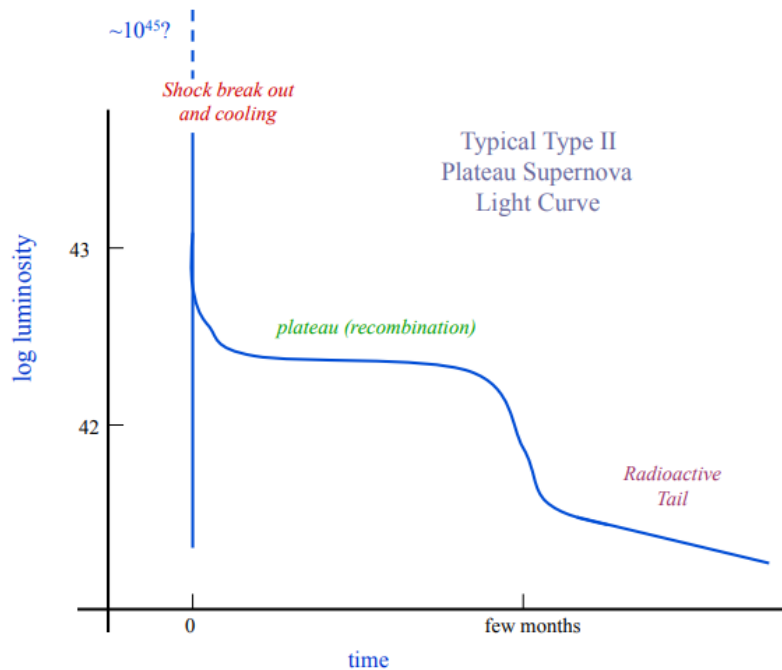
77d



γ -ray emission

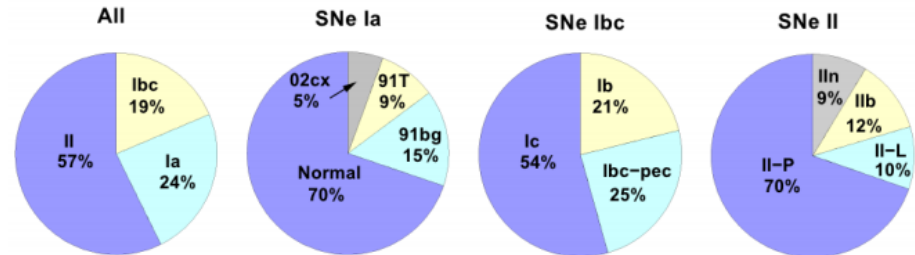
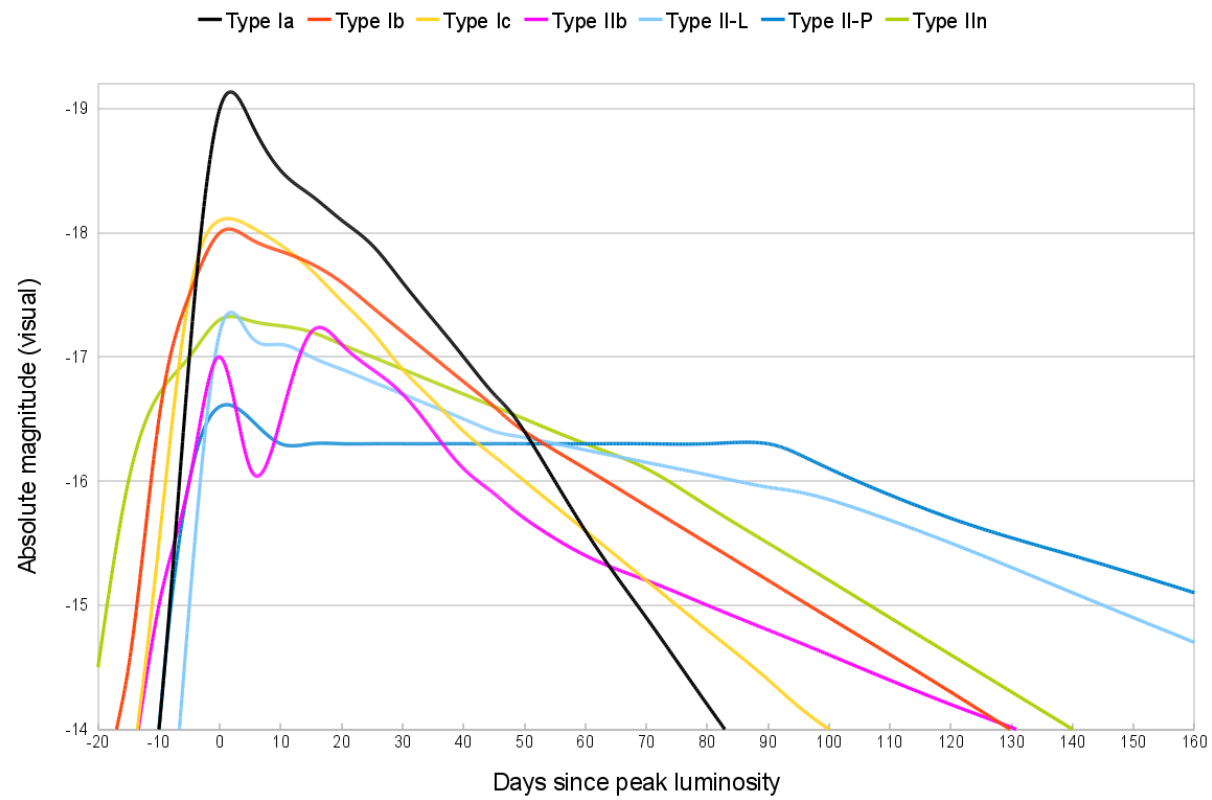


Type II Supernovae Lightcurve



- **Break out** – temperatures of 100's of thousands K. Very brief stage, not observed so far (indirectly in 87A). Shock heating followed by expansion and cooling
- **Plateau** – the hydrogen envelope expands and cools to ~ 5500 K. Radiation left by the shock is released. Nearly constant luminosity (T is constant and radius of photosphere does not change much – around 10^{15} cm). Lasts until the entire envelope recombines.
- **Radioactive tail** – powered by the decay of radioactive ^{56}Co produced in the explosion as ^{56}Ni .

Core collapse Supernovae Lightcurve



Synthesis of radioactive isotopes in supernovae

Short-lived isotopes: $^{56,57}\text{Ni}$ (all), ^{44}Ti (SN II and Ib/c; also in sub-Chandra SN Ia), ^{60}Co (SN II and Ib/c)

- diagnostic of models: observation of **individual objects**
- **γ -ray lines:** $^{56,57}\text{Ni}$ and ^{44}Ti yields (better in SN Ia; detected in SN 1987A)
 - bolometric light curves

Long-lived isotopes: ^{26}Al and ^{60}Fe (SN II and Ib/c)

- diagnostic of models: observation of **accumulated emission in the Galaxy**

γ -ray line astronomy could provide crucial insights on supernova models

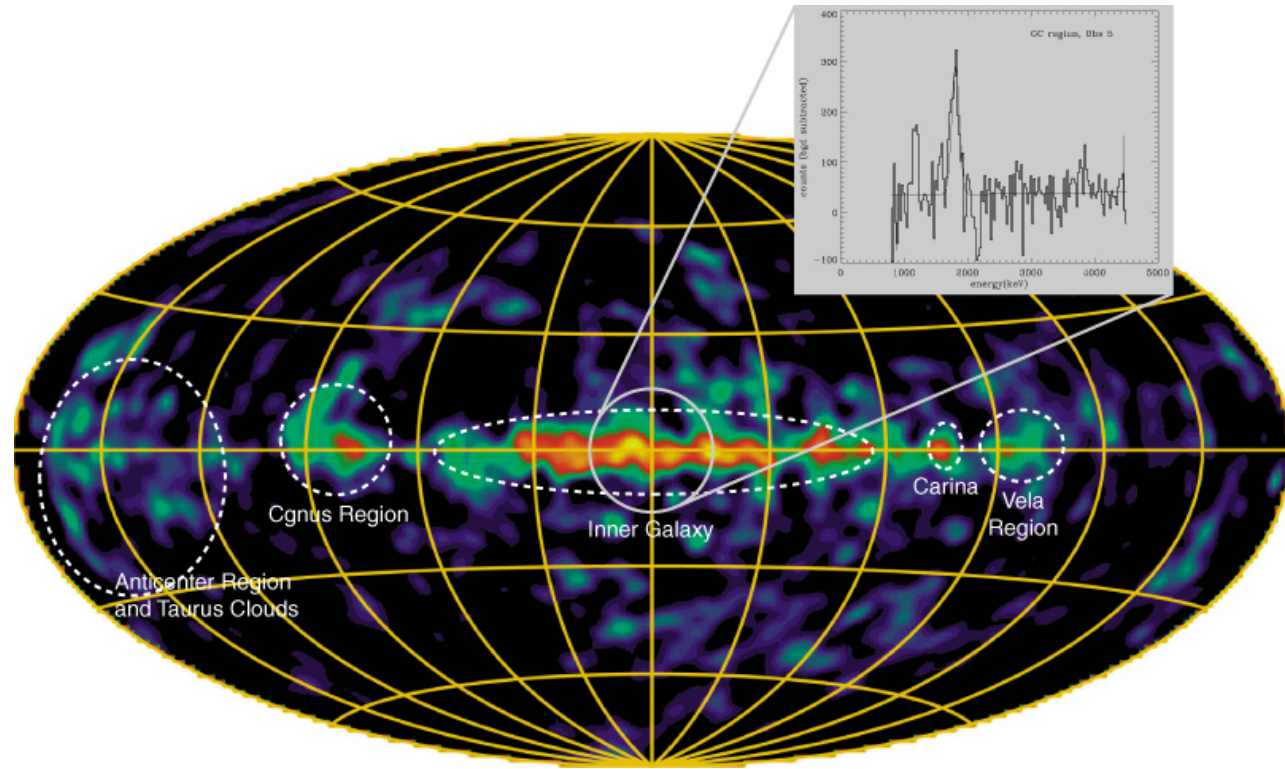
Emission Lines via Radioactive Decay

Decay chain	Mean life (years)	$Q/Q(^{56}\text{Ni})$	γ -ray energy (MeV)
$^{56}\text{Ni} \rightarrow ^{56}\text{Co} \rightarrow ^{56}\text{Fe}$	0.31	1	0.847
			1.238
$^{57}\text{Co} \rightarrow ^{57}\text{Fe}$	1.1	2×10^{-2}	0.122
			0.014
$^{22}\text{Na} \rightarrow ^{22}\text{Ne}$	3.8	5×10^{-3}	1.275
			0.068
$^{44}\text{Ti} \rightarrow ^{44}\text{Sc} \rightarrow ^{44}\text{Ca}$	68	2×10^{-3}	1.156
			0.078
			0.068
$^{60}\text{Fe} \rightarrow ^{60}\text{Co} \rightarrow ^{60}\text{Ni}$	4.3×10^5	1.5×10^{-4}	1.332
			1.173
			0.059
$^{26}\text{Al} \rightarrow ^{26}\text{Mg}$	1.1×10^6	1.5×10^{-4}	0.85 (e^+)

Quick decay,
must be
searched
within few days
from the SN
explosion

Longer decay time, can diffuse in
the interstellar medium, can be
searched long after SN event.

Emission Lines via Radioactive Decay: Aluminium-26



Gamma Ray line for Iron 60

Detection of γ -ray lines from interstellar ^{60}Fe by the high resolution spectrometer SPI

M.J. Harris¹, J. Knödseder¹, P. Jean¹, E. Cisana², R. Diehl³, G.G. Lichti³, J.-P. Roques¹, S. Schann¹ and G. Weidenspointner¹

¹ Centre d'Étude Spatiale des Rayonnements, B.P. N° 4346, 31028 Toulouse Cedex 4, France

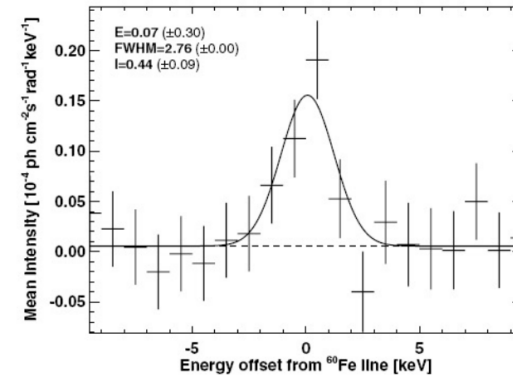
² IASF, Via E. Bassini 15, 20133 Milano, Italy

³ Max-Planck-Institut für extraterrestrische Physik, Postfach 1603, 85740 Garching, Germany

⁴ DSM/DAPNIA /Sap, CEA Saclay, 91191 Gif-sur-Yvette, France

Received

Abstract. It is believed that core-collapse supernovae (CCSN), occurring at a rate \sim once per century, have seeded the interstellar medium with long-lived radioisotopes such as ^{60}Fe (half-life 1.5 Myr), which can be detected by the γ -rays emitted when they β -decay. Here we report the detection of the ^{60}Fe decay lines at 1173 keV and 1333 keV with fluxes $3.7 \pm 1.1 \times 10^{-5} \text{ } \gamma \text{ cm}^{-2} \text{ s}^{-1}$ per line, in spectra taken by the SPI spectrometer on board *INTEGRAL* during its first year. The same analysis applied to the 1809 keV line of ^{26}Al yielded a line flux ratio $^{60}\text{Fe}/^{26}\text{Al} = 0.11 \pm 0.03$. This supports the hypothesis that there is an extra source of ^{26}Al in addition to CCSN.



INTEGRAL/SPI

Wang et al., A&A, 2007

^{26}Al vs. ^{60}Fe production in core collapse supernovae

^{60}Fe is produced by n-capture on $^{56,58}\text{Fe}$ in the O-Ne burning shell and in the base of the He burning shell

- ^{26}Al and ^{60}Fe are coproduced in the same regions within SN II

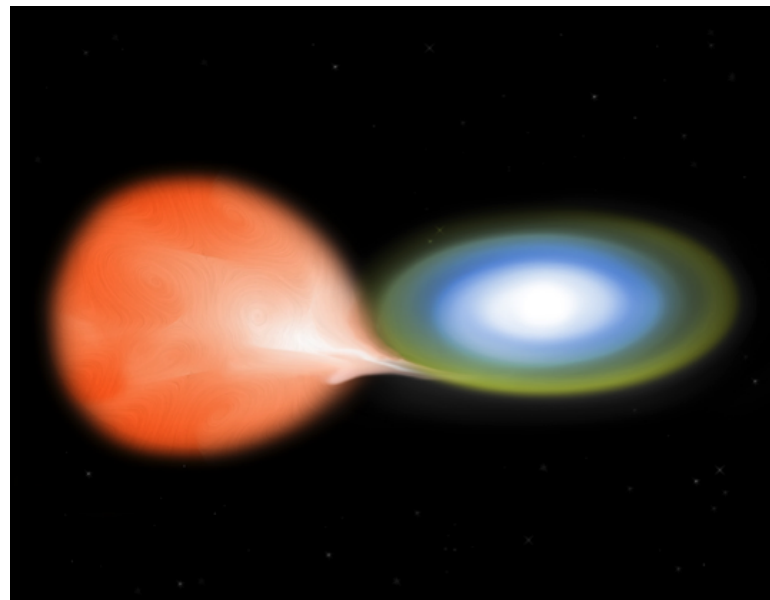


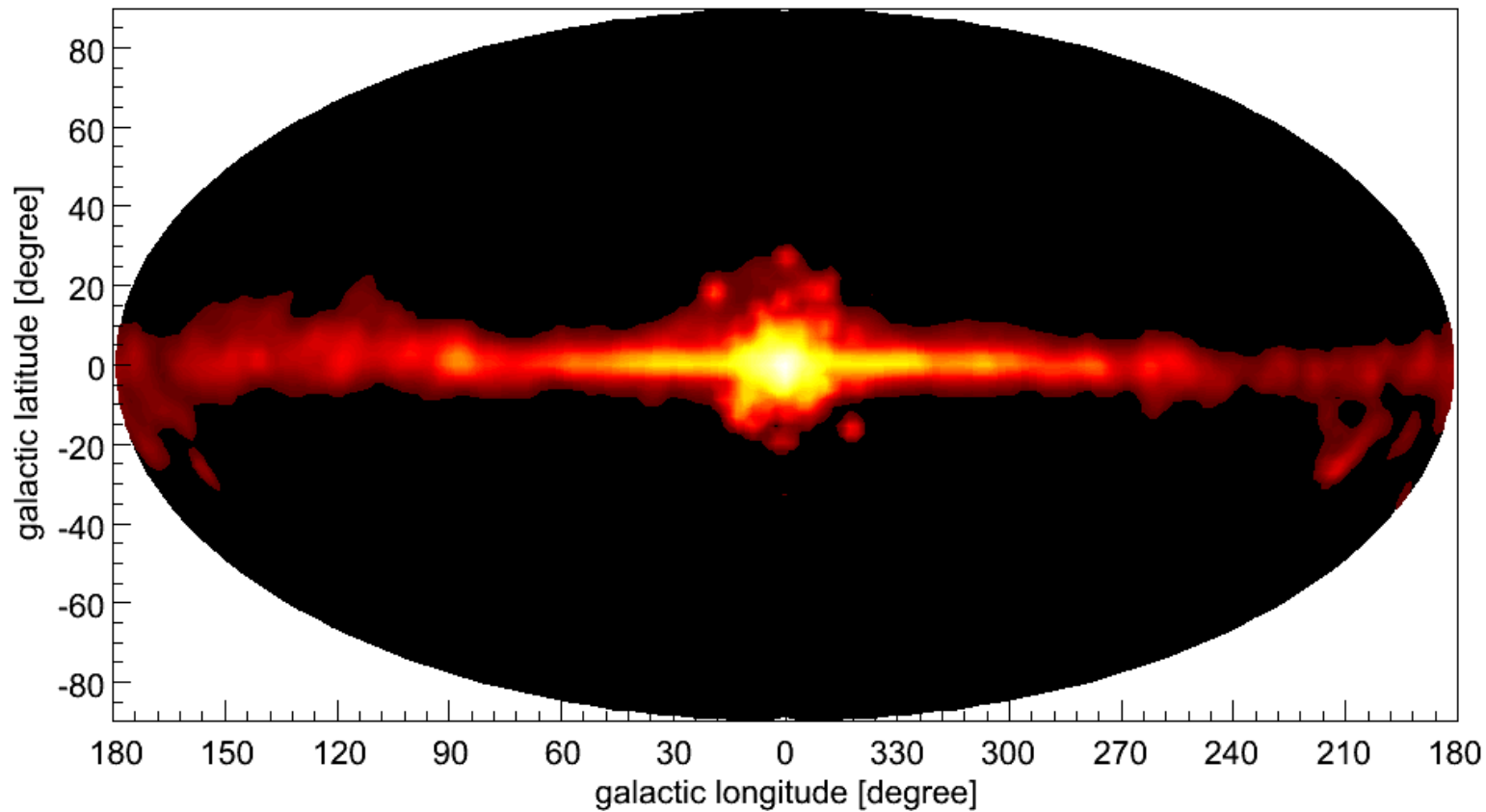
similar spatial distributions in supernovae ejecta

- Typical yields: $^{26}\text{Al} \approx 10^{-4} M_{\odot}$, $^{60}\text{Fe} \approx 4 \cdot 10^{-5} M_{\odot}$

Gamma Ray Lines in Novae

Novae are cataclysmic variables exhibiting explosions due to thermonuclear burning. Gamma-rays are expected from positron-electron annihilation (511 keV), and gamma-ray lines at 478 keV (Be-7 decay in CO novae, lifetime 77 days) and 1275 keV (Na-22 decay in ONe novae, lifetime 3.75 years).





Electron-Positron Annihilation and the
511 keV line

Where do Positrons come from?

1. e^+ are created in β^+ from unstable nuclei: nucleosynthesis or interaction of cosmic rays with ISM (InterStellar Medium)
2. pion decay: interaction of cosmic rays with ISM
3. e^+/e^- pair production around compact objects: pulsars, jets in black hole binaries, etc.
4. Exotic channels: dark matter
5. Supermassive black hole in the Galactic Center.

Where do Positrons come from?

1. e^+ are created in β^+ from unstable nuclei: nucleosynthesis or interaction of cosmic rays with ISM (InterStellar Medium)

Isotope	Decay chain	Lifetime	Line energy (keV)
^{56}Ni	$^{56}\text{Ni} \rightarrow ^{56}\text{Co}$	8.8 d	158, 812, 750, 480
^{56}Co	$^{56}\text{Co} \rightarrow ^{56}\text{Fe}$	111 d	847, 1238
^{57}Ni	$^{57}\text{Ni} \rightarrow ^{57}\text{Co} \rightarrow ^{57}\text{Fe}$	(52 h) 390 d	122
^{44}Ti	$^{44}\text{Ti} \rightarrow ^{44}\text{Sc} \rightarrow ^{44}\text{Ca}$	89 y (5.4 h)	78, 68, 1157
^{26}Al	$^{26}\text{Al} \rightarrow ^{26}\text{Mg}$	1.0×10^6 y	1809
^{60}Fe	$^{60}\text{Fe} \rightarrow ^{60}\text{Co} \rightarrow ^{60}\text{Ni}$	2.0×10^6 y (7.6 y)	1173, 1332
^7Be	$^7\text{Be} \rightarrow ^7\text{Li}$	77d	478
^{22}Na	$^{22}\text{Na} \rightarrow ^{22}\text{Ne}$	3.8 y	1275

Supernovae mainly

Novae mainly


\rightarrow electron capture

\rightarrow inverse beta (e^+)

\rightarrow beta decay (e^-)

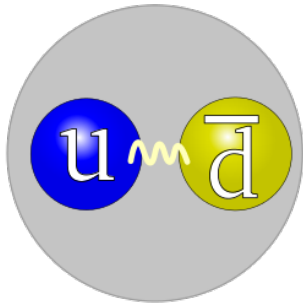
Where do Positrons come from?

1. e^+ are created in β^+ from unstable nuclei: nucleosynthesis or interaction of cosmic rays with ISM (InterStellar Medium)

- ^{56}Co (^{56}Ni) (supernova explosions, SNe) $\sim 10^{43} e^+/s$ 
- ^{44}Sc (^{44}Ti) (SNe) $\sim 2 \times 10^{42} e^+/s$
- ^{26}Al (SNe, WR (Wolf Rayet), AGB (giant stars), novae) $\sim 2 \times 10^{42} e^+/s$
- ^{22}Na (nova explosions) $\sim (0.5-2) \times 10^{41} e^+/s$
 $\langle E(e^+) \rangle \sim 1 \text{ MeV}$

Where do Positrons come from?

2. pion decay: interaction of cosmic rays with ISM



$$\begin{aligned}\pi^+ &: u\bar{d} \\ \pi^0 &: u\bar{u} \text{ or } d\bar{d} \\ \pi^- &: d\bar{u}\end{aligned}$$

Pions are hadrons (bound states of quarks) and mesons (bound states of quark/anti-quark)

Cosmic rays can interact with atoms in the ISM. Sometimes this interaction produces pions.

Pions decay after a short time via different channels.

Example:

$$\begin{aligned}\pi^+ &\rightarrow \mu^+ + \nu_\mu \quad (\tau = 2,6 \cdot 10^{-8} \text{ s}) \\ &\quad \downarrow \\ &\rightarrow e^+ + \nu_e + \bar{\nu}_\mu \quad (\tau = 2,2 \cdot 10^{-6} \text{ s})\end{aligned}$$

$$\pi^0: p + p \rightarrow X + \pi^0 \rightarrow 2\gamma \rightarrow e^-e^+ (\tau = 1.8 \times 10^{-16} \text{ s})$$

Where do Positrons come from?

3. e^+/e^- pair production around compact objects: pulsars, jets in black hole binaries, etc.

Pair production around compact objects is mainly driven by photon decay.

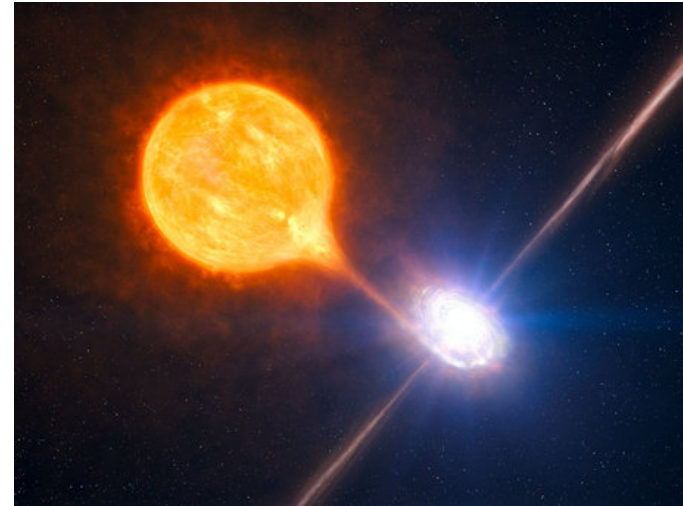
A photon can decay into a positron-electron pair (pair production) when in a strong magnetic field, or close to a nucleus (conservation of energy/momentum):

$$\gamma \rightarrow e^- + e^+$$

These conditions occur often around pulsars, but also in jets around black holes and neutron stars in general, in AGNs and in GRBs.

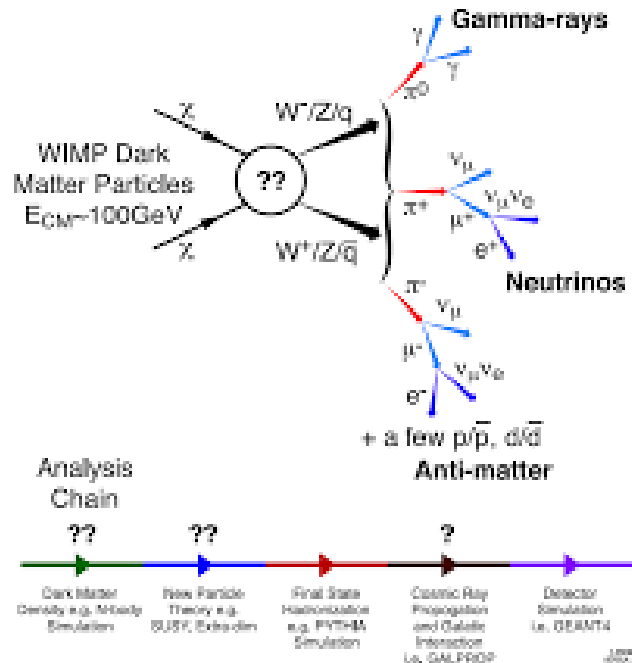
For example, 1E1740.7-2942, or the **Great Annihilator**, is a microquasar (black hole accreting binary with a strong jet). The jet is probably emitting synchrotron radiation from positron-electron pairs streaming out at high velocities from the source of antimatter.

Antimatter is present because we see a strong 511 keV signal.



Where do Positrons come from?

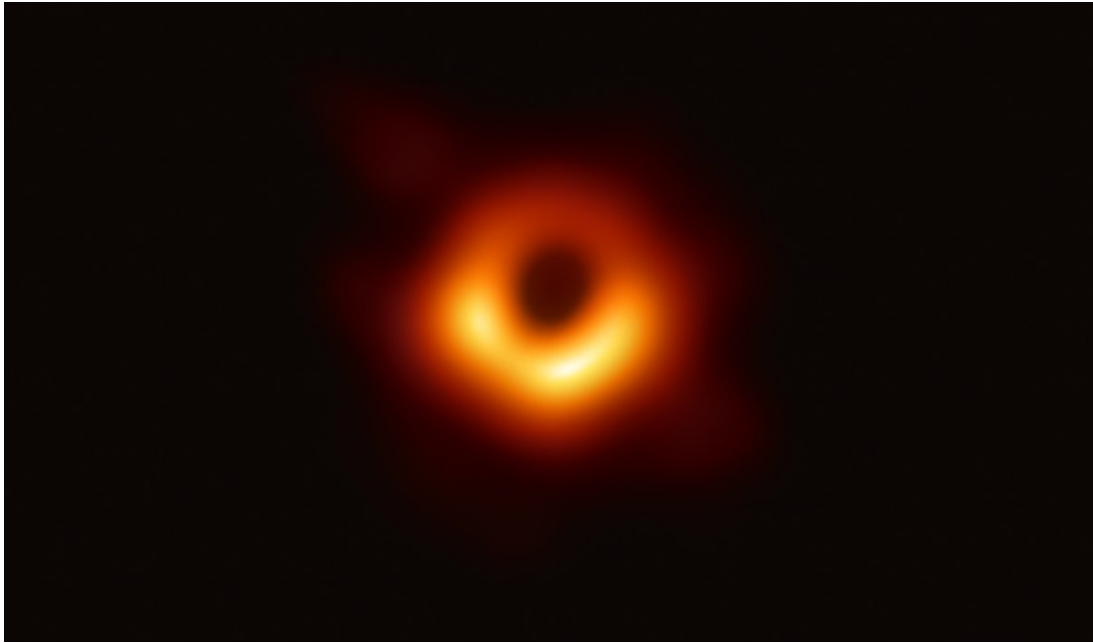
4. Exotic channels: dark matter



Several Dark Matter processes predict the existence of a halo that might produce the 511 keV line via WIMP processes.

Where do Positrons come from?

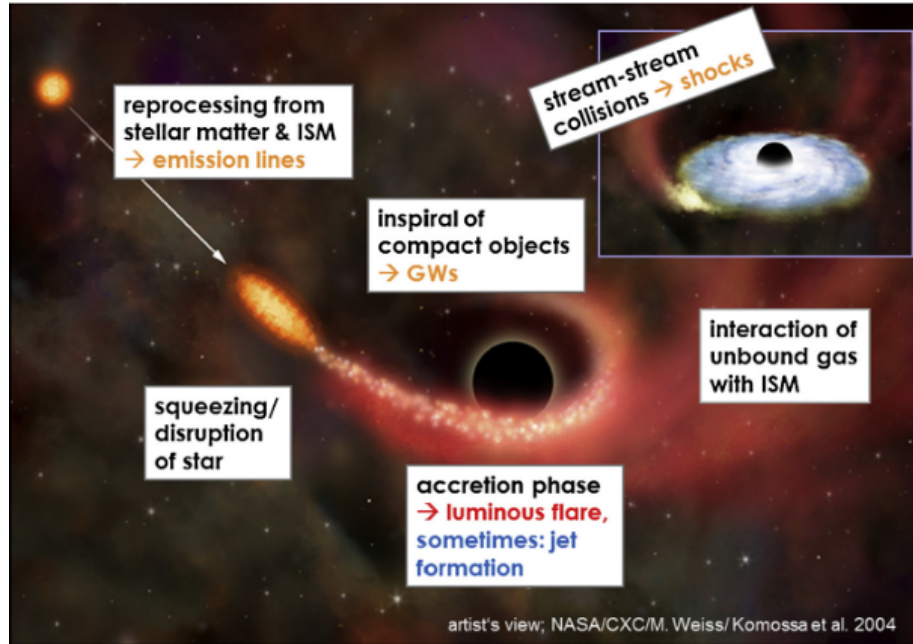
5. Supermassive black hole in the Galactic Center.



The SMBH in the GC might have been active in the last ~ 10 Myr (about 1,000-10,000x its current activity), with a sudden turn off around 300 yr ago. This might have been due to the passage of the shell of the SN SGR A-East. If true, this might have generated a large flow of p^+ , created close to the event horizon

Where do Positrons come from?

5. Supermassive black hole in the Galactic Center.



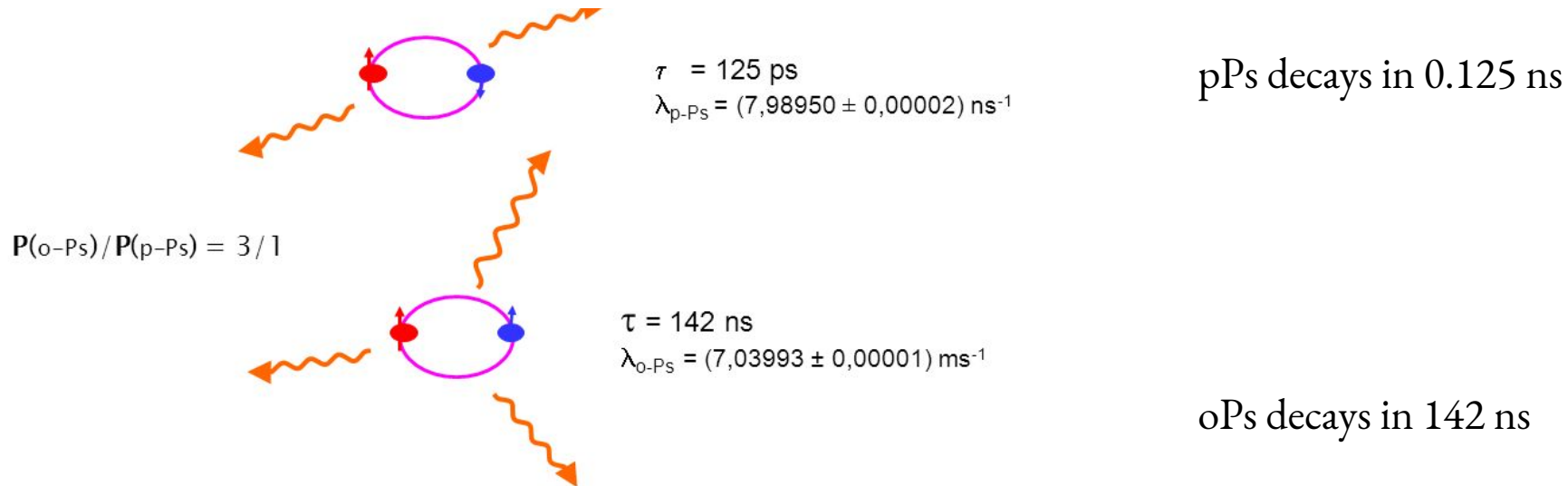
Alternative: Tidal Disruption Events

Estimated rate: $1/(10,000-100,000 \text{ yr})$

[Note: only “small” SMBHs can tidally disrupt a star. Only tiny ($<10^5 \text{ Msun}$) black holes can disrupt a white dwarf. Why?]

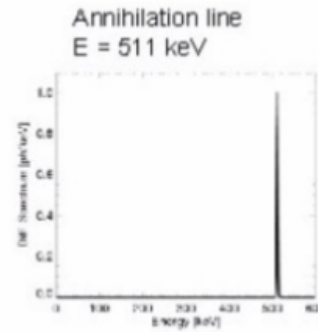
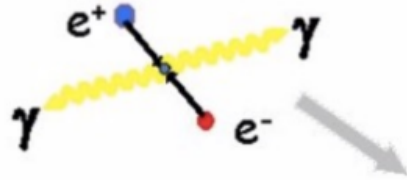
para-Positronium (pPs) and ortho-Positronium (oPs)

Positronium is a metastable *onium* (i.e., a bound state formed by a particle and its anti-particle). After a radioactive atom in a material undergoes a β^+ decay (positron emission), the resulting high-energy positron slows down by colliding with atoms, and eventually annihilates with one of the many electrons in the material. It may however first form positronium before the annihilation event.

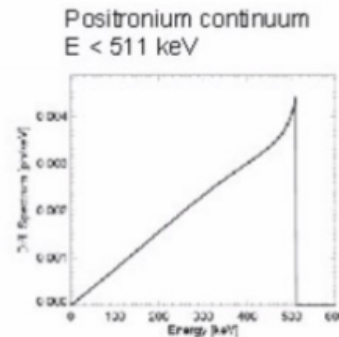
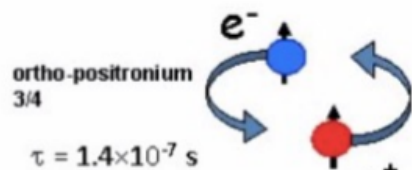
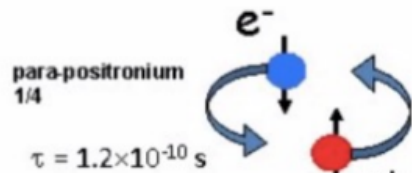


How does Positronium decay?

- Direct annihilation



- Annihilation via positronium (Ps) formation



Two channels, depending on whether it is *para* (singlet) or *ortho* (triplet).

pPs creates sharp 511 keV line.
oPs creates a broad continuum below 511 keV.

Detection of pair annihilation

THE ASTROPHYSICAL JOURNAL, 184: 103–125, 1973 August 15

© 1973. The American Astronomical Society. All rights reserved. Printed in U.S.A.

The line at 511 keV longest known and most studied extra-solar γ -ray line A γ -ray line at $E < 0.5$ MeV was first detected from the direction of the GC, with a scintillator detector (NaI) onboard a balloon, thus with poor energetic resolution (Johnson & Haymes 1973): RICE experiments

DETECTION OF A GAMMA-RAY SPECTRAL LINE FROM THE GALACTIC-CENTER REGION

W. N. JOHNSON III* AND R. C. HAYMES

Department of Space Science, Rice University, Houston, Texas

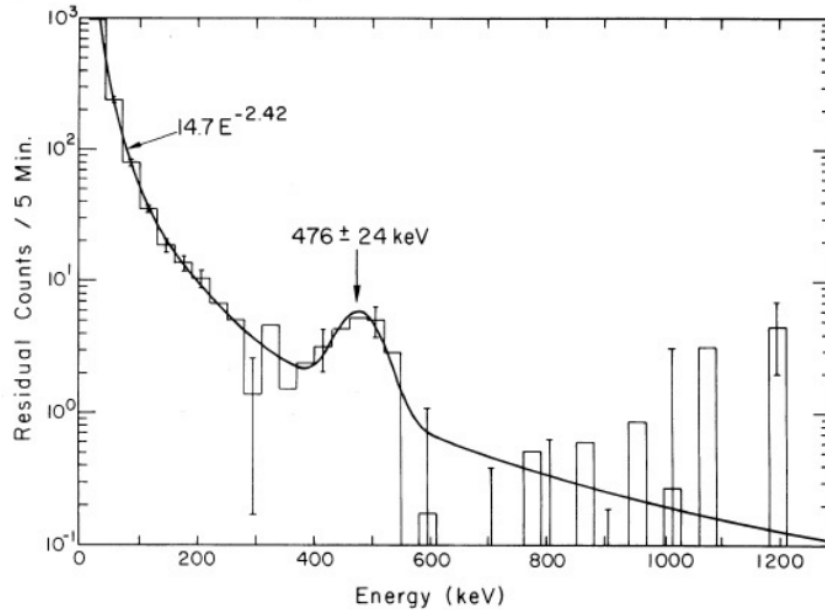
Received 1973 January 23; revised 1973 March 28

ABSTRACT

A balloon-borne experiment timed to observe a lunar occultation of the X-ray source GX 3+1 was conducted on 1971 November 20, from Paraná, Argentina. Good data were obtained in the 30 keV–2.4 MeV energy band with two 24° FWHM instruments for over four hours, including the hour-long occultation. The observed spectra confirm our 1970 measurements of a spectral line superposed on a power-law continuum radiated from the galactic-center region. The combination of the 1970 and 1971 data places the line 5.3 standard deviations above the continuum. The line energy is 476 ± 24 keV; its intensity is $(1.8 \pm 0.5) \times 10^{-3}$ photons $\text{cm}^{-2} \text{s}^{-1}$. A result of the occultation observation is that, while it is ruled out as the origin of the bulk of the radiation from the galactic center region, a relatively faint, hard-exponential continuum is radiated by GX 3+1, a result in agreement with an extrapolation of that measured at lower energies by the LRL group. The identification of the source of the 476-keV radiation is unclear, although there was a 2.3 standard deviation decrease in the spectral line during the occultation.

Subject headings: galactic nuclei — gamma rays — lunar occultation

Detection of pair annihilation



Johnson & Haymes 1973

Line is broad and not centered around 511 keV due to the very poor NaI detector resolution.

Detection of pair annihilation

In 1977, observations with Ge detectors
(higher energetic
resolution) were performed: narrow line with
 $E=511 \text{ keV}$
(Leventhal et al. 1978).
Interpretation of lower E resolution
experiments:
511 keV line convolved with Ps continuum

DETECTION OF 511 keV POSITRON ANNIHILATION RADIATION FROM THE GALACTIC CENTER DIRECTION*

M. LEVENTHAL

Bell Laboratories, Murray Hill, New Jersey

AND

C. J. MACCALLUM† AND P. D. STANG†

Sandia Laboratories, Albuquerque

Received 1978 June 7; accepted 1978 July 6

ABSTRACT

A balloon-borne germanium γ -ray telescope was flown over Alice Springs, Australia, in an attempt to detect spectral features from the galactic center (GC) direction. A 511 keV positron annihilation line was detected at a flux level of $(1.22 \pm 0.22) \times 10^{-3} \text{ photons s}^{-1} \text{ cm}^{-2}$. Suggestive evidence for the detection of the three-photon positronium (ps) continuum is presented. A brief discussion of the possible origin of the positrons is given.

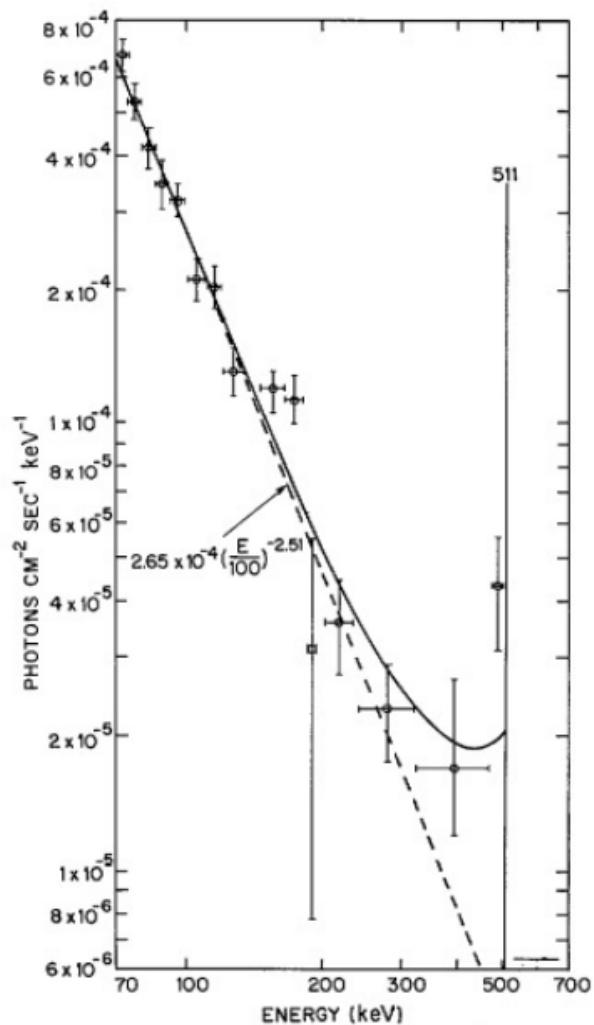


FIG. 2a.—Differential photon spectrum for the target direction GC at the top of the atmosphere. The solid line is a least-squares fit to the data as discussed in the text. The parameter f was found to be 0.92.

*Leventhal
et al. 1978*

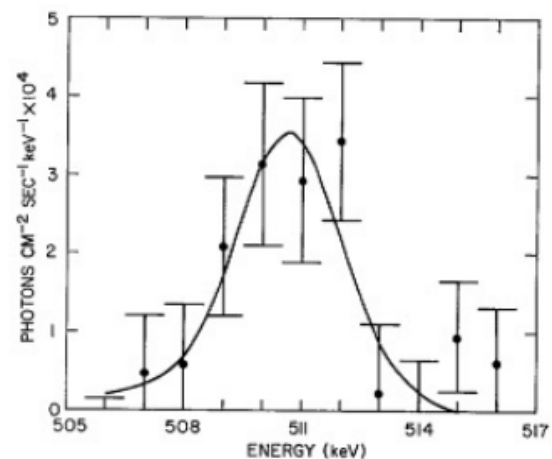


FIG. 2b.—An expanded version of Fig. 2a in the vicinity of 511 keV. The line center was found at 510.7 ± 0.5 keV with a width limited by system resolution at ≤ 3.2 keV. The line flux was found to be $(1.22 \pm 0.22) \times 10^{-3}$ photons $\text{cm}^{-2}\text{s}^{-1}$ at the top of the atmosphere.

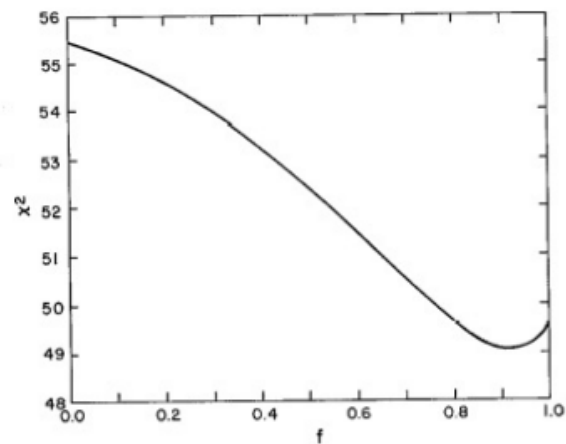
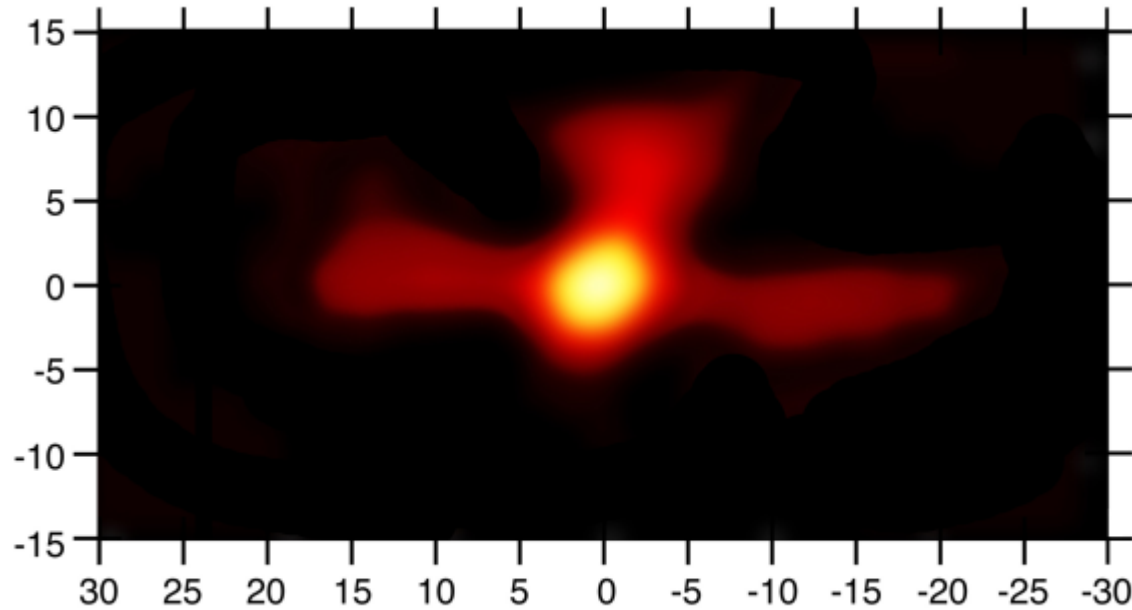


FIG. 3.— χ^2 versus f , the fraction of positrons annihilating via the ps state. For 57 degrees of freedom and five parameters.

CGRO/OSSE map of the 511 keV emission

central bulge + galactic plane + positive latitude enhancement



Purcell et al., 1997

Fluxes(10^{-4} phot/cm²/s)

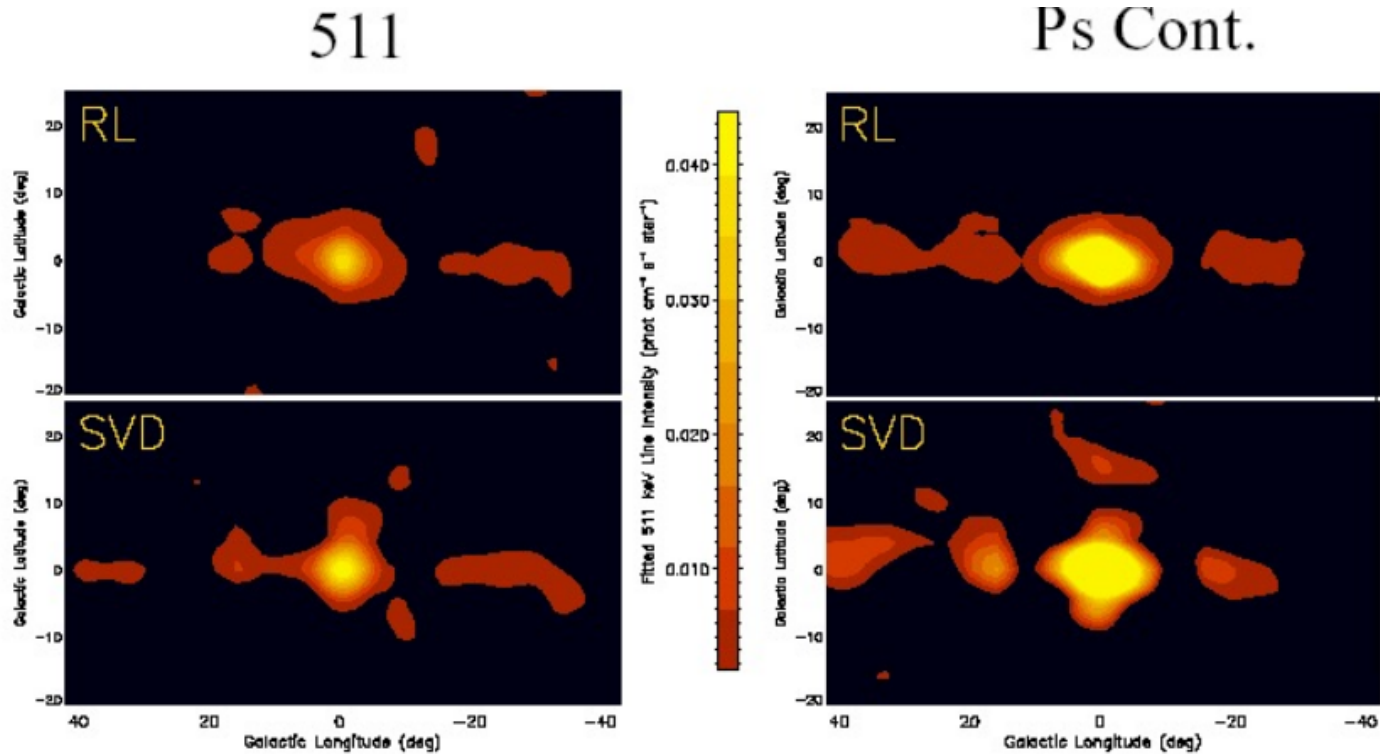
central bulge: 3.3 (size 4 deg)

Galactic plane: 10 (size lat.~12 deg., long.~30 deg.)

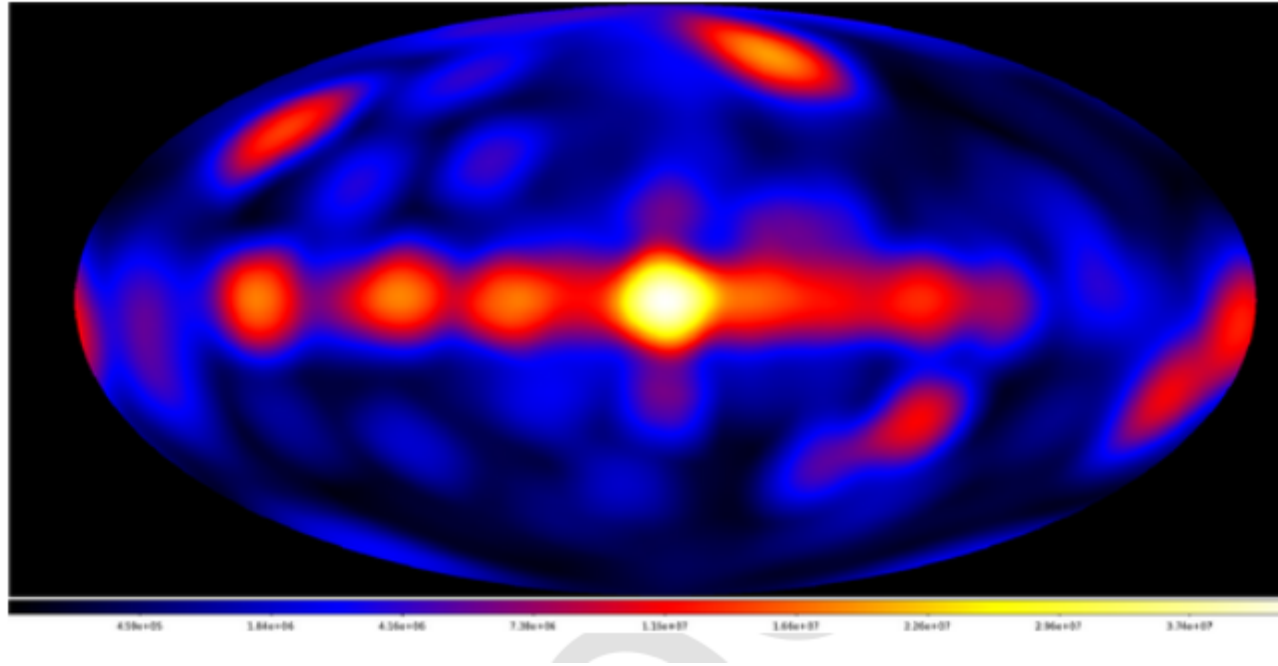
Positive-latitude excess: 9 (~16 deg.; centroid b~12 deg., l~-2 deg.).

No time variability

CGRO/OSSE map of the 511 keV emission



INTEGRAL/SPI map of the 511 keV emission



511 keV line components

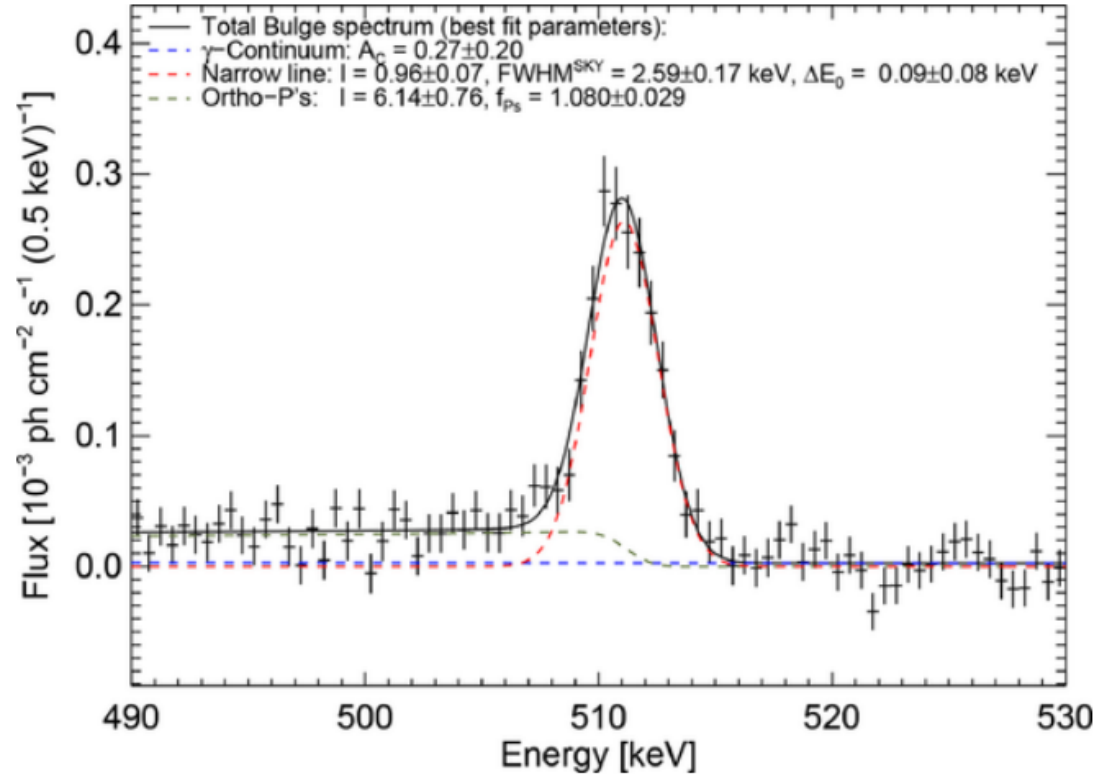


Fig. 14. Total Bulge spectrum approximated with a Gaussian line, Ortho-positronium emission and a power law continuum. Adapted from Siegert (2016).

Positrons energy losses

As charged leptons, positrons interact via the electromagnetic force with all basic constituents of the ISM, namely, electrons, ions, atoms, molecules, solid dust grains, photons, and magnetic fields. Since their initial kinetic energy is generally larger than the kinetic energy of the targets in the ISM, positrons lose energy in these interactions. The energy loss rate and the kind of interaction depend on the energy of positrons and the density of target particles.

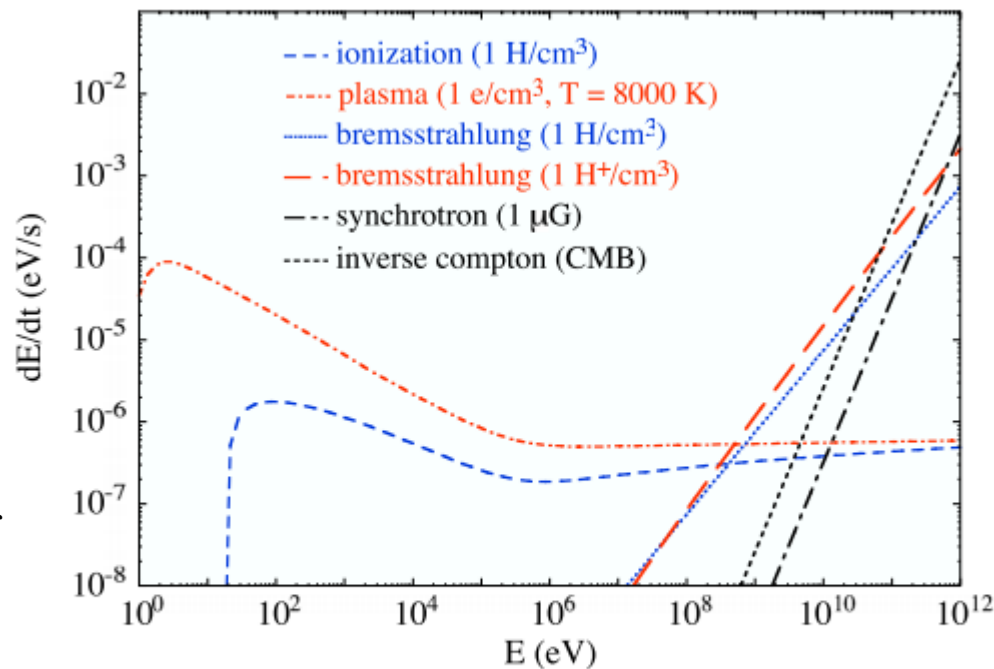


FIG. 23 (color online). Energy loss rate for positrons in ISM conditions. For synchrotron losses, the pitch angle is taken as $\pi/2$.

Positrons energy losses example: $E > 10$ GeV (IC)

Ultrarelativistic positrons ($E > 10$ GeV) lose their energy mainly by inverse-Compton scattering with cosmic microwave background (CMB) photons and interstellar radiation fields. When the interaction occurs with an isotropic photon gas in the Thomson scattering regime, the energy loss rate (in eV/s) can be calculated from:

$$P_{IC} \propto -U_{rad} \gamma^2 \beta^2$$

The radiation energy density depends on the position of the positron in the Galaxy; it ranges from 0.26 eV/cm³ (CMB) to 11.4 eV/cm³ in the Galactic center region

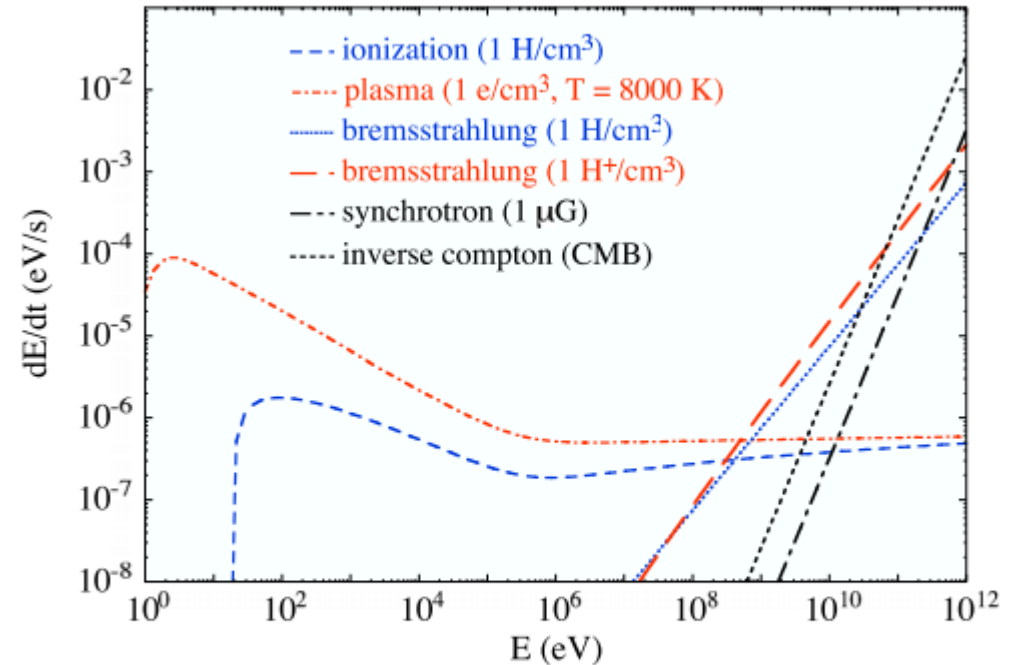


FIG. 23 (color online). Energy loss rate for positrons in ISM conditions. For synchrotron losses, the pitch angle is taken as $\pi/2$.

From Prantzos et al. 2011

Positrons energy losses example: $E > 10$ GeV (Synchrotron)

If the magnetic field is considerable (larger than $B > 6.3 \mu G \sqrt{U_{rad}}$) then synchrotron losses dominate over IC (again for $E > 10$ GeV).

$$P_{synch} \propto -U_B \gamma^2 \beta^2$$

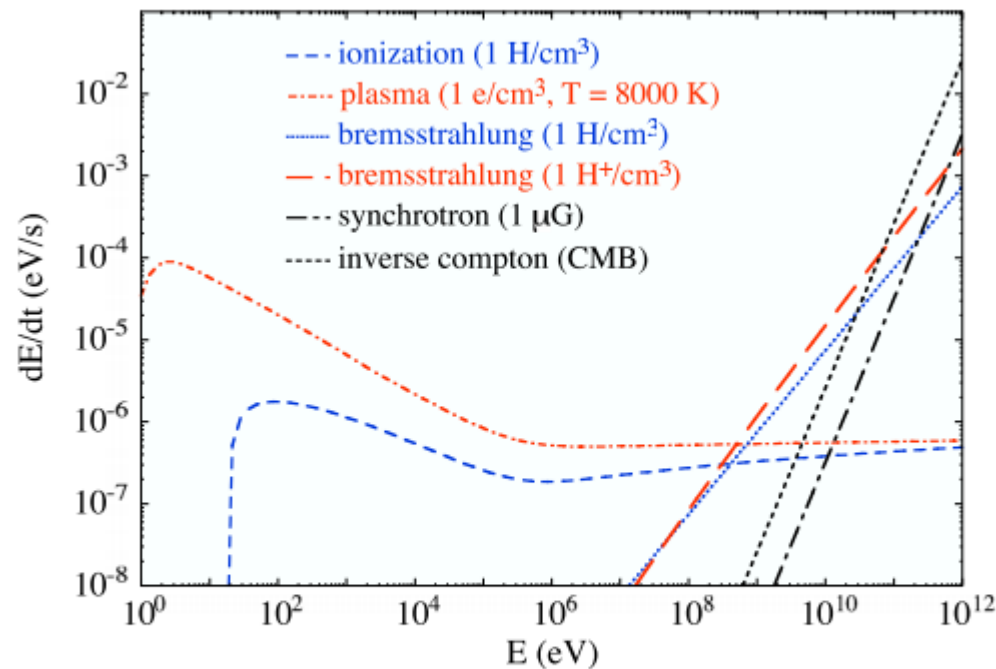


FIG. 23 (color online). Energy loss rate for positrons in ISM conditions. For synchrotron losses, the pitch angle is taken as $\pi/2$.

Positrons energy losses example: 1–10 GeV (Bremsstrahlung)

In the 1–10 GeV energy range, positrons lose their energy mainly by emitting bremsstrahlung radiation in interactions with ions, electrons, and atoms. The energy loss rate depends on the target mass, charge, and density.

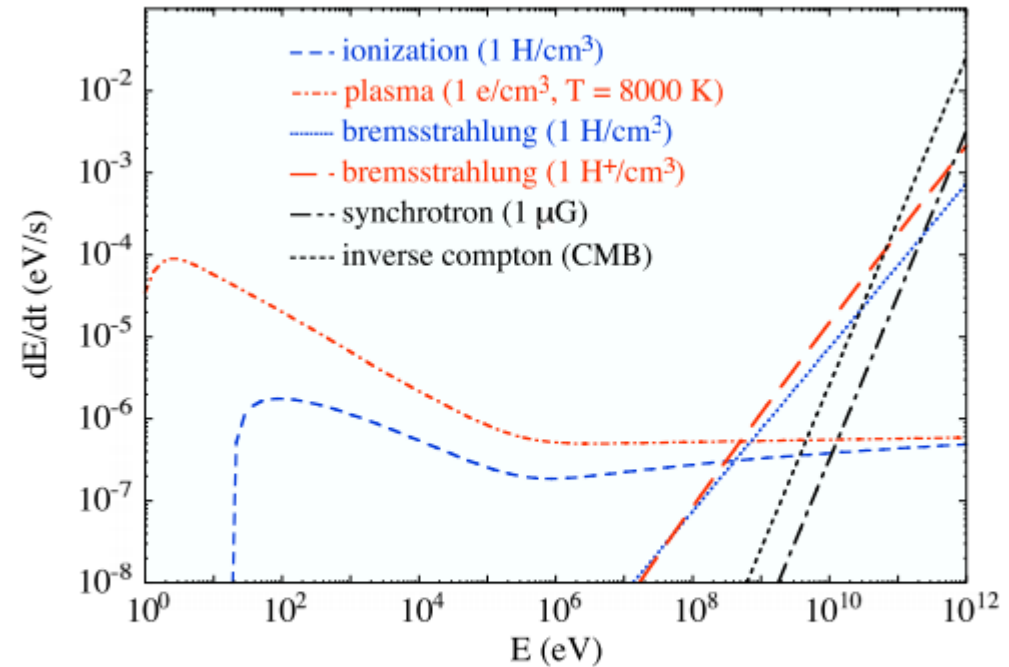


FIG. 23 (color online). Energy loss rate for positrons in ISM conditions. For synchrotron losses, the pitch angle is taken as $\pi/2$.

From Prantzos et al. 2011

Positrons energy losses example: <1 GeV (Coulomb & inelastic scattering)

Below 1 GeV, positrons lose their energy mainly via Coulomb scatterings with free electrons and/or inelastic interactions with atoms and molecules. The former process is a continuous energy loss, whatever the energy of positrons. At high energy, the target electrons can be considered at rest and the energy loss rate depends mostly on their density

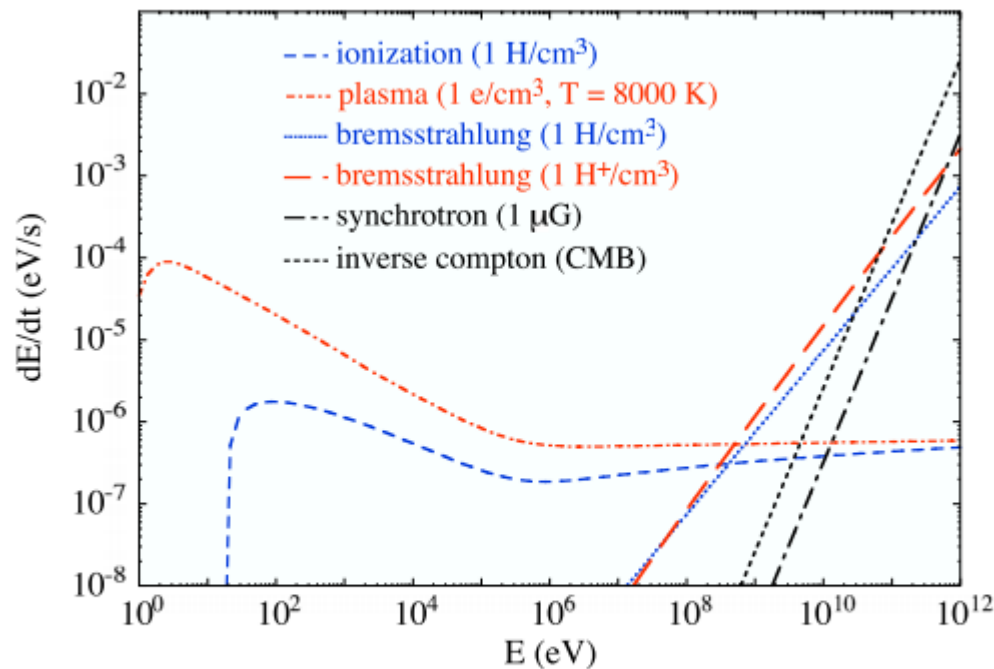


FIG. 23 (color online). Energy loss rate for positrons in ISM conditions. For synchrotron losses, the pitch angle is taken as $\pi/2$.

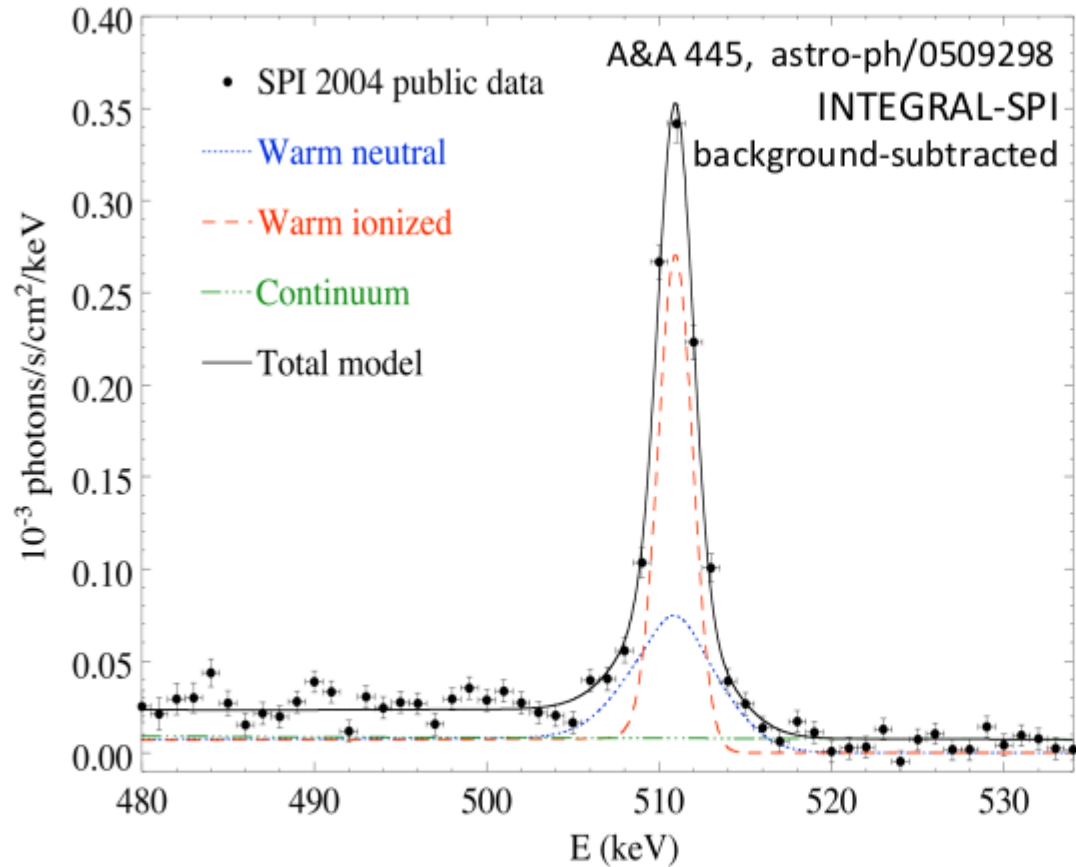
Positrons energy losses: Thermalization

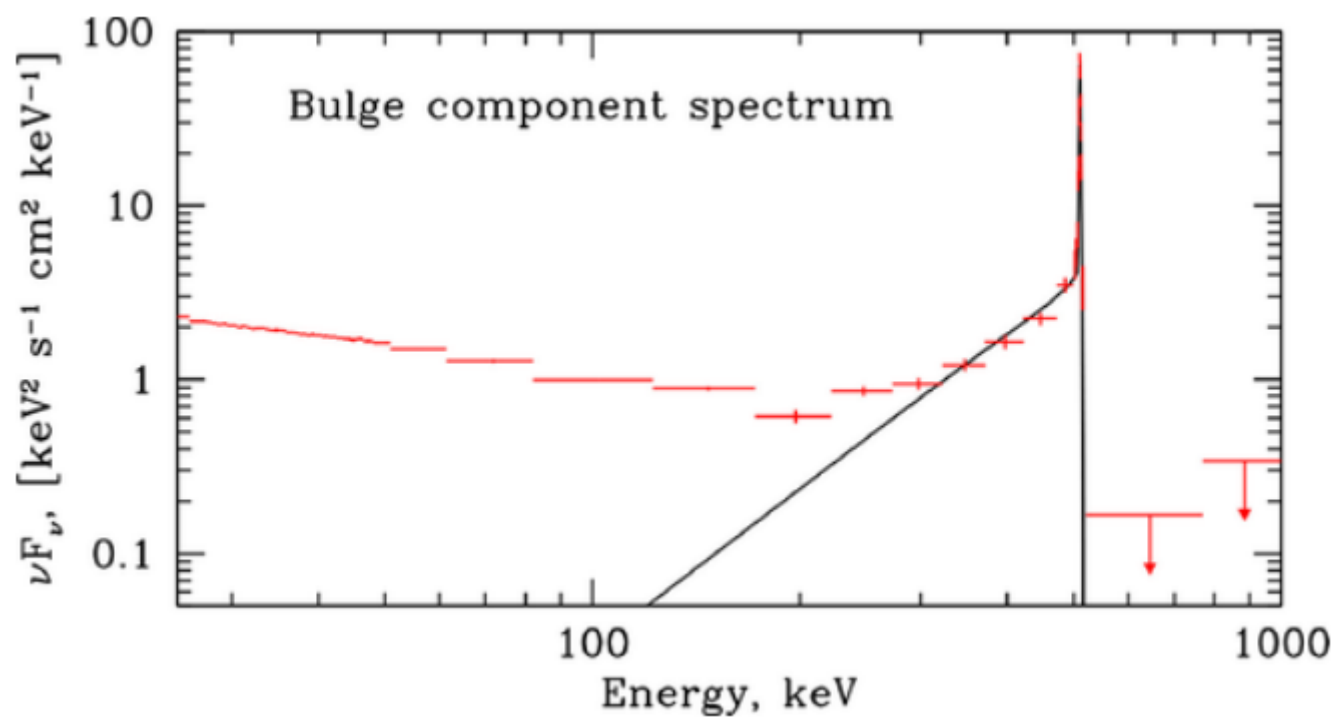
Once the positrons have come down to energies similar to those of the ambient medium, they start to “thermalize,” i.e., their energy distribution relaxes to the Maxwellian function which characterizes the interstellar gas (or plasma). The ISM usually consists of a few phases, each with rather well-defined physical characteristics (temperature, density, ionization fraction); The time scale needed for the energetic positrons to relax to the ISM Maxwellian distribution is compared to the time scale for subsequent annihilation processes; if the former time scale is longer than the latter, it would be incorrect to assume a Maxwellian distribution for both the positrons and the ISM when calculating the e^+ annihilation rates.

TABLE IV. Physical properties (typical temperatures, hydrogen densities, and ionization fractions) of the different ISM phases in the Galactic disk.

Phase	T (K)	n_H (cm^{-3})	x_{ion}
Molecular (MM)	10–20	10^2 – 10^6	$\lesssim 10^{-4}$
Cold neutral (CNM)	20–100	20–100	4×10^{-4} – 10^{-3}
Warm neutral (WNM)	10^3 – 10^4	0.2–2	0.007–0.05
Warm ionized (WIM)	~ 8000	0.1–0.3	0.6–0.9
Hot ionized (HIM)	$\sim 10^6$	0.003–0.01	1

Effect of ISM on 511 keV line





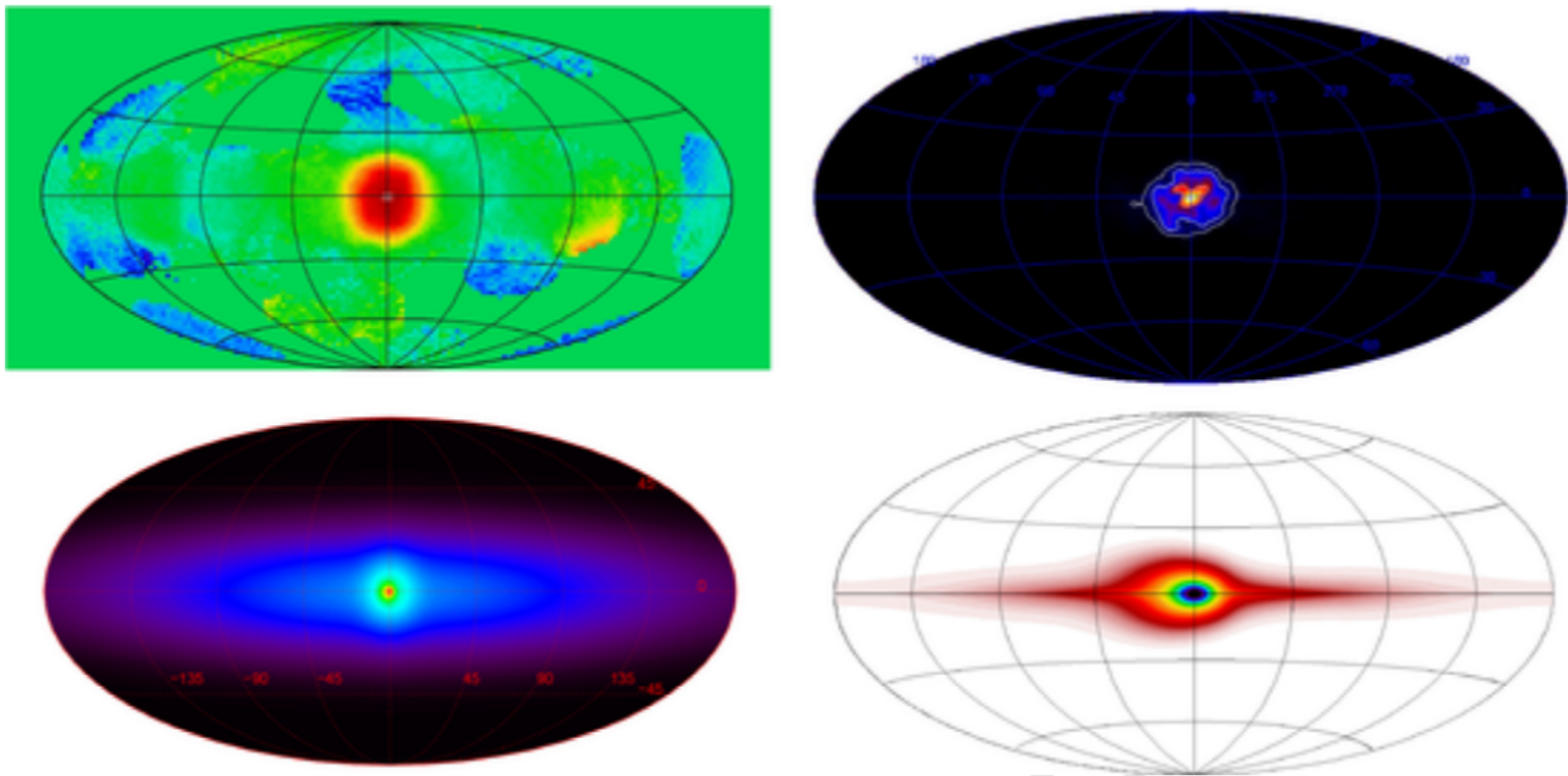
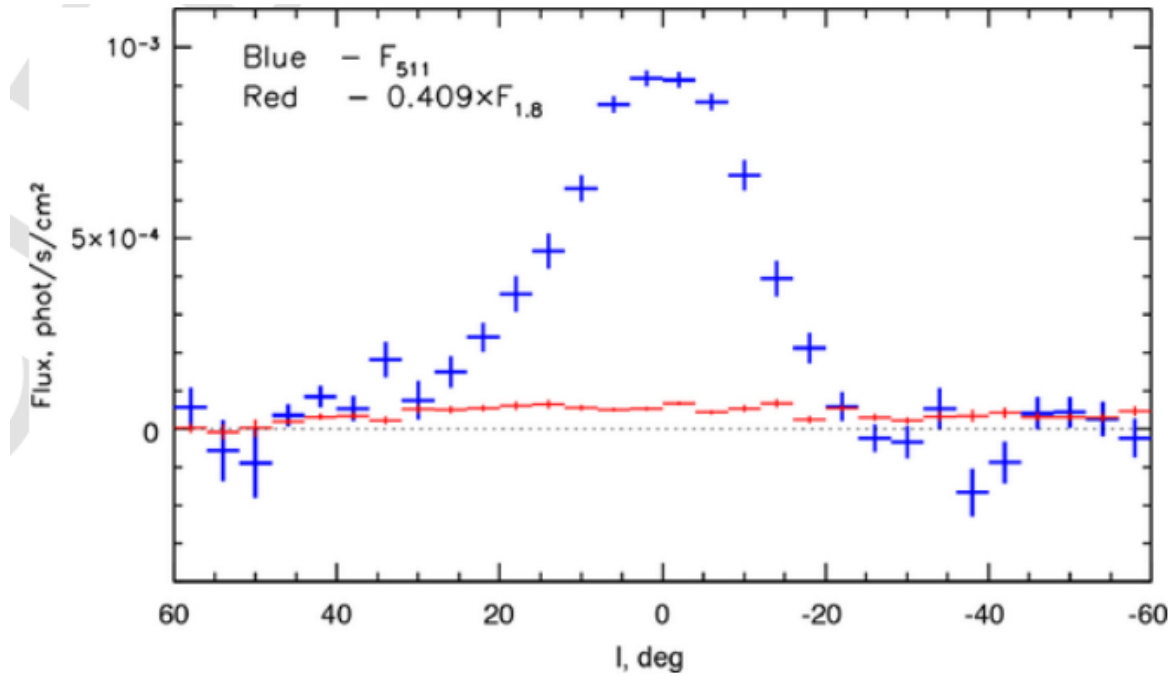


Fig. 6. All-sky maps of the 511 keV line emission obtained using different methods. **Top-left:** Light-bucket map using the data collected in Feb-Nov 2003 (Churazov et al., 2005, unpublished). Only the central component (red) is significant. Blue and green regions are consistent with zero within uncertainties. **Top-right:** A map based on the Lucy-Richardson reconstruction algorithm (after 17 iterations) using the data obtained before 2004 (Knödlseider, 2005). **Bottom-left:** A map based on fitting the data with an analytic model, consisting of a Narrow Bulge, Broad Bulge and a Disk using the data up to April 2013 (Siegert, 2016). **Bottom-right:** A map based on fitting the amplitudes of the Bulge and Disk templates, reflecting the distribution of stars in the Galaxy (Churazov et al., 2011). The templates are based on the 3D models of 2MASS star counts (López-Corredoira et al., 2005). All models agree on the presence of the bright central component, while the constraints on the exact properties of the extended disk component (or on the substructure in the bulge) are weaker.



Al-26 insufficient to explain the observed flux.

Churazov et al. 2011

Fig. 9. Expected contribution of positrons produced by ^{26}Al decay to the annihilation line flux in the vicinity of the GC. The light-bucket technique was used. The slice has a width of 16° perpendicular to the Galactic plane and is centred at $b = 0$. The step along the Galactic plane is 4° . The measured flux in the 508-514 keV band is shown with blue crosses; the red crosses show the flux in the 1804-1813 keV band scaled by a factor of 0.409, which is the expected 511 keV line flux arising from ^{26}Al decay under the assumption that 100 per cent of positrons annihilate through the formation of positronium. Clearly, the 1804-1813 keV flux arising from the GC region is far too low to explain the observed 511 keV line by the local ^{26}Al decay. Adapted from Churazov et al. (2011).

High Bulge/Disk Ratio needs a source of positrons

Knödlseider et al. 2005

The most distinctive morphological feature of the 511 keV emission is the large B/D luminosity ratio of $3 - 9$. Unless there is a mechanism that strongly suppresses positron annihilation in the galactic disk, or that somehow transports positrons from the disk into the galactic bulge or halo where they annihilate, the positron source population we are seeking for should also exhibit such a high B/D ratio.

High Bulge/Disk Ratio needs a source of positrons

511 keV γ -rays more concentrated at the galactic "bulge" than any other λ Positrons are produced in β + decays of SN ejecta (^{56}Ni , ^{44}Ti , ^{26}Al) BUT: bulge/disk luminosity does not match ($\times 4$)
distribution of galactic SN \implies need for exotic source? (e.g. dark matter)

Solution 1: at least half of the e^+ may originate in a class of binary systems via γ - γ interactions in the accretion disk (Nature 451)

Solution 2: significant e^+ propagation before slowing down and annihilating (ApJ 698)

LETTERS

An asymmetric distribution of positrons in the Galactic disk revealed by γ -rays

Georg Weidenspointner^{1,2,3}, Gerry Skinner^{1,4,5}, Pierre Jean¹, Jürgen Knödseder¹, Peter von Ballmoos¹, Giovanni Bignami^{1,8}, Roland Diehl², Andrew W. Strong², Bertrand Cordero⁶, Stéphane Schanne⁶ & Christoph Wi

Gamma-ray line radiation at 511 keV is the signature of electron–positron annihilation. Such radiation has been known for 30 years to come from the general direction of the Galactic Centre¹, but the origin of the positrons has remained a mystery. Stellar nucleosynthesis^{2–4}, accreting compact objects^{5–8}, and even the annihilation of exotic dark-matter particles⁹ have all been suggested. Here we report a distinct asymmetry in the 511-keV line emission coming from the inner Galactic disk (~ 10 – 50° from the Galactic Centre). This asymmetry resembles an asymmetry in the distribution of low mass X-ray binaries with strong emission at photon energies >20 keV ('hard' LMXBs), indicating that they may be the dominant origin of the positrons. Although it had long been suspected that electron–positron pair plasmas may exist in X-ray binaries, it was not evident that many of the positrons could escape to lose energy and ultimately annihilate with electrons in the interstellar medium and thus lead to the emission of a narrow 511-keV line. For these models, our result implies that up to a few times 10^{41} positrons escape per second from a typical hard LMXB. Positron production at this level from hard LMXBs in the Galactic bulge would reduce (and possibly eliminate) the need for more exotic explanations, such as those involving dark matter.

Nature, 2008

Solution 1

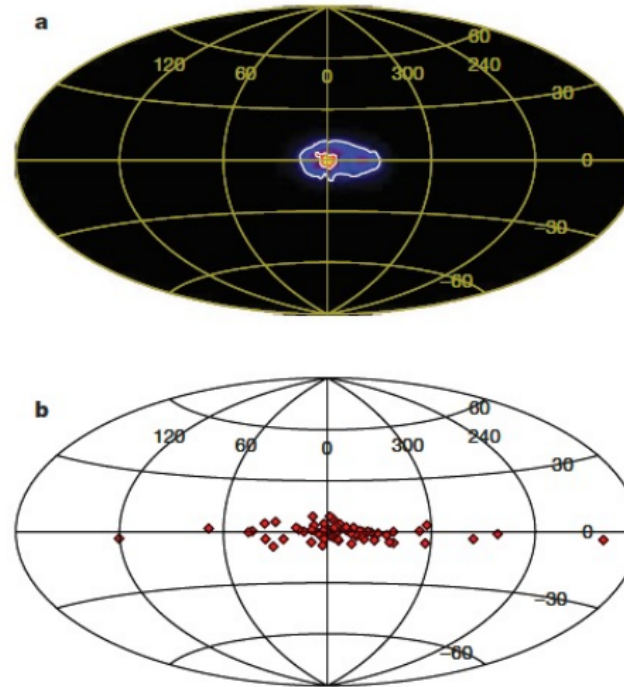
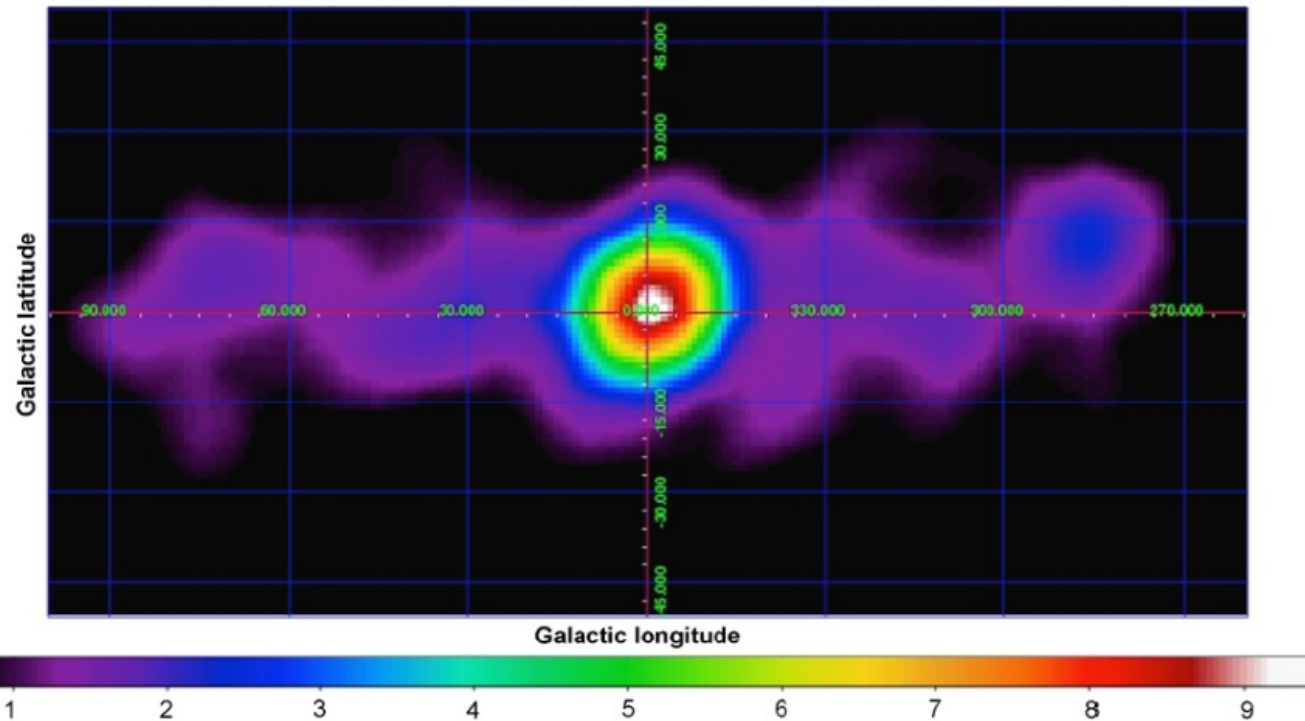


Figure 1 | A sky map in the 511-keV electron–positron annihilation line, and the sky distribution of hard LMXBs. In both maps, the Galactic Centre is at the origin, the Galactic plane is along the equator; Galactic longitude and latitude are shown in degrees. **a**, The 511-keV line map. The bright bulge region is prominent, as is the distinct asymmetry in the flux from the inner disk; contours correspond to intensity levels of 10^{-3} and 10^{-2} photons $\text{cm}^{-2} \text{s}^{-1} \text{sr}^{-1}$. The map is based on observations with the



BUT different result as well possible

Criticism to Solution 1

Fig. 3 Spatial distribution of the 511 keV positron annihilation emission in the Galactic Centre. Long INTEGRAL exposures show a dominant central bulge and surprisingly weak emission from the disk. Although an earlier analysis was interpreted in terms of an asymmetry in the disk (Weidenspointner et al. 2008), a more recent one is shown here, as a significance map of the electron-positron annihilation emission in the 508 to 514 keV range, using data from six years of observation. It uses an alternative background modeling technique (Bouchet et al. 2010), suggesting that if any asymmetry is present, it is more likely associated with an offset of the bulge. Clearly, more observations are needed to understand the precise morphology and so provide key clues as to the origin of the positrons and how and where they annihilate (Figure adapted from Bouchet et al. 2010)

Is There a Dark Matter Signal in the Galactic Positron Annihilation Radiation?

R. E. Lingenfelter,¹ J. C. Higdon,^{2,*} and R. E. Rothschild¹

¹*Center for Astrophysics and Space Sciences, University of California San Diego, La Jolla, California 92093, USA*

²*Keck Science Center, Claremont Colleges, Claremont, California 91711-5916, USA and California Institute of Technology, Pasadena, California 91125, USA*

(Received 6 April 2009; revised manuscript received 14 May 2009; published 17 July 2009)

Assuming Galactic positrons do not go far before annihilating, a difference between the observed 511 keV annihilation flux distribution and that of positron production, expected from β^+ decay in Galactic iron nucleosynthesis, was evoked as evidence of a new source and signal of dark matter. We show, however, that the dark matter sources cannot account for the observed positronium fraction without extensive propagation. Yet with such propagation, standard nucleosynthetic sources can fully account for the spatial differences and positronium fraction, leaving no new signal for dark matter to explain.

**Criticism
to
Solution 2**

Monte Carlo modelling of the propagation and annihilation of nucleosynthesis positrons in the Galaxy

A. Alexis^{1,2}, P. Jean^{1,2}, P. Martin^{1,2}, and K. Ferrière^{1,2}

Results. Regardless of the Galactic magnetic field configuration and the escape fraction chosen for ^{56}Ni positrons, the 511 keV intensity distributions are very similar. The main reason is that $\sim\text{MeV}$ positrons do not propagate very far away from their birth sites in our model. The direct comparison to the data does not allow us to constrain the Galactic magnetic field configuration and the escape fraction for ^{56}Ni positrons. In any case, nucleosynthesis positrons produced in steady state cannot explain the full annihilation emission. The comparison to the data shows that (a) the annihilation emission from the Galactic disk can be accounted for; (b) the strongly peaked annihilation emission from the inner Galactic bulge can be explained by positrons annihilating in the central molecular zone, but this seems to require more positron sources than the population of massive stars and type Ia supernovae usually assumed for this region; (c) the more extended emission from the Galactic bulge cannot be explained. We show that a delayed 511 keV emission from a transient source, such as a starburst episode or a recent activity of Sgr A*, occurring between 0.3 and 10 Myr ago and producing between 10^{57} and 10^{60} sub-MeV positrons could explain this extended component, and potentially contribute to the inner bulge signal.

Positron annihilation signatures associated with the outburst of the microquasar V404 Cygni

Thomas Siegert¹, Roland Diehl¹, Jochen Greiner¹, Martin G. H. Krause^{1,2}, Andrei M. Beloborodov³, Marion Cadolle Bel⁴, Fabrizia Guglielmetti¹, Jerome Rodriguez⁵, Andrew W. Strong¹ & Xiaoting Zhang¹

Microquasars^{1–4} are stellar-mass black holes accreting matter from a companion star⁵ and ejecting plasma jets at almost the speed of light. They are analogues of quasars that contain supermassive black holes of 10^6 to 10^{10} solar masses. Accretion in microquasars varies on much shorter timescales than in quasars and occasionally produces exceptionally bright X-ray flares⁶. How the flares are produced is unclear, as is the mechanism for launching the relativistic jets and their composition. An emission line near 511 kiloelectronvolts has long been sought in the emission spectrum of microquasars as evidence for the expected electron–positron plasma. Transient high-energy spectral features have been reported in two objects^{7,8}, but their positron interpretation⁹ remains contentious. Here we report observations of γ -ray emission from the microquasar V404 Cygni during a recent period of strong flaring activity¹⁰. The emission spectrum around 511 kiloelectronvolts shows clear signatures of variable positron annihilation, which implies a high rate of positron production.

This supports the earlier conjecture that microquasars may be the main sources of the electron–positron plasma responsible for the bright diffuse emission of annihilation γ -rays in the bulge region of our Galaxy¹¹. Additionally, microquasars could be the origin of the observed megaelectronvolt continuum excess in the inner Galaxy.

controversial paper

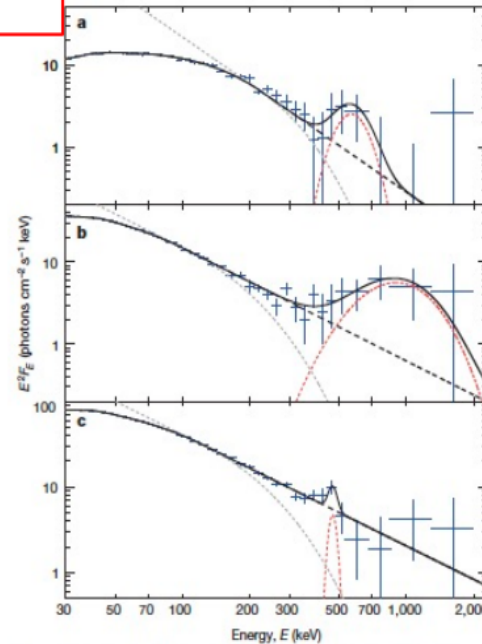


Figure 1 | Spectral evolution of V404 Cygni. a–c, Spectra in the soft γ -ray band in three different flaring epochs (a–c show the spectra measured in INTEGRAL orbits 1554, 1555 and 1557, corresponding to epochs 1, 2 and 3, respectively). Data (blue; error bars, 1 s.d.) are fitted as the sum of the Comptonization continuum (black dashed curve) and annihilation radiation from a relativistic hot plasma (red dashed curve). The standard thermal Comptonization model (grey dashed curve) fits the data up to ~ 200 keV; it declines exponentially at higher energies and falls short of the observed flux. Our conservative, modified continuum model follows a power law instead. E , energy; F_E , flux at energy E .


Alternatives?

From Motta et al 2021:
“Independent studies have failed to confirm this 511 keV line detection. Such a discrepancy was likely caused by the event selection of the SPI data, which is a particularly important issue for bright sources”

[Published: 04 July 2017](#)

Can Flare Stars Explain the Annihilation Line from the Galactic Bulge?

Alternatives?

[G. S. Bisnovatyi-Kogan](#)  & [A. S. Pozanenko](#)

[Astrophysics](#) **60**, 223–227 (2017) | [Cite this article](#)

48 Accesses | **6** Citations | [Metrics](#)

We consider the low-mass flare stars which form the bulk of the population in the galactic bulge as a source of the positrons needed to form the observed narrow annihilation line from the galactic bulge. Estimates based on the observed flares in low-mass stars, together with observations of the annihilation line in solar flares, show that the rate of production of positrons in flares in the stars in the bulge may be sufficient to explain the formation of the narrow stationary annihilation line observed from the region of the galactic bulge.

Summary of Special Relativistic Effects

	Space Interval	Time Interval	Power
Rods & Clocks	$L = \frac{L'}{\gamma}$	$\Delta t_e = \Delta t'_e \gamma$	$P = P'$
Photons	$\Lambda = L' \delta \sin \theta$	$\Delta t_a = \frac{\Delta t'_e}{\delta}$	$P = P'$

$K \rightarrow$ Lab frame

$K' \rightarrow$ Rest frame

subscript “a” \rightarrow arrival

subscript “e” \rightarrow emission

Other important transformations:

Solid angle $d\Omega = \frac{d\Omega'}{\delta^2}$	Specific Intensity $I_\nu = I'_\nu \delta^3$	Intensity $I = I' \delta^4$	Energy $E = E' \delta$
--	---	--------------------------------	---------------------------

Summary of Radiation Properties: Continuum

	Thermal	Blackbody	Bremsstr.	Synchrotron	Inverse Compton	Curvature Radiation
<i>Optically thick</i>	–	YES	NO	–	–	–
<i>Maxwellian distribution of velocities</i>	YES	YES	–	NO	–	NO
<i>Relativistic speeds</i>	–	–	–	YES	YES	YES
<i>Main Properties</i>	Matter in thermal equilibrium	Matter AND radiation in thermal equilibrium	Radiation emitted by accelerating particles	Radiation emitted by accelerated particles in B field.	Relativistic electron/photon collisions	Radiation emitted by accelerated particles along the parallel B field component

Summary of Radiation Properties: Lines

	Absorption	Emission	From
Atomic transition	Hydrogen (e.g., Balmer lines)	H_{α} , $Fe K_{\alpha}$	Accretion Disks
Gamma-decay	–	Al-26, Fe-60, Co-56, Ti-44	Supernovae
Matter-antimatter annihilation	–	511 keV line + continuum	e-/e+ pair annihilation (direct, oPs, pPs)

Summary of Supernovae

Type	Mechanism	Hydrogen lines	Compact Object Formation
Ia	Single-degenerate (WD accretion) or double-degenerate (WD-WD merger)	No	None
Ib	Core-collapse	No/Very weak	NS/BH. Possible relation to GRBs
Ic	Core-collapse	No	NS/BH. Possible relation to GRBs
II	Core-collapse	Yes	NS/BH

Summary on Supernova Remnants

	Ambient medium	Ejecta	Shock	Duration
1. Free Expansion	Mass swept up by forward shock \ll ejecta mass	supersonic expansion	Forward shock – Reverse shock formation	~few hundreds years
2. Adiabatic Expansion	Mass swept up by forward shock $>$ ejecta mass	supersonic expansion	Reverse shock disappears	~10,000 years
3. Radiative Phase	significant cooling	deceleration	forward shock significantly decelerates	~100,000 years
4. Dispersion to ISM				~ millions of years